Universidade Nova de Lisboa

Faculdade de Ciências e Tecnologia

Departamento de Conservação e Restauro

Spectroscopy Studies on Conservation Issues in Modern and Contemporary Paintings

Joana Andreia Lameiras Domingues

Dissertation presented to the Faculty of Sciences and Technology of New University of Lisbon in fulfilment of the requirements for the Master's degree in Conservation and Restoration

Specialization in easel painting

Supervisor: Prof. Dr. Costanza Miliani (CNR-ISTM)

Co-Supervisor: Dr. Francesca Rosi (SMAArt)

2010

Acknowledgements

I am deeply thankful to my supervisor, Prof. Costanza Miliani, whose encouragement and guidance had been essential for the development of this thesis.

It was an honour for me to do my training stage with the SMAArt working group, an opportunity given by Prof. Bruno Brunetti, to whom I owe my deepest gratitude.

I would also like to show my sincere gratitude to Francesca and Brenda for all the help on the bench and portable equipments, and also those colleagues from SMAArt and CNR-ISTM that supported me from the beginning.

Finally, I would like to thank the kind collaboration from Vivi Pouli, (FORTH-IESL) and Grazia De Cesare (ISCR).

This thesis would not have been possible if it wasn't the support of my family and friends. I would like to particularly show my heartily gratitude to my mother, who has always been there for me, and also to my friend and colleague Vanessa Otero, whose support and help really made the difference.

Sumário

A pintura de arte contemporânea é um dos grandes desafios da conservação-restauro de bens culturais. Algumas destas pinturas contêm repintes de composição química semelhante à das camadas pictóricas originais, colocando em causa a reversibilidade dos mesmos.

Neste trabalho a microscopia óptica e as espectroscopias de FTIR e Raman foram utilizadas para avaliar a eficácia e o dano associados às limpezas química e a laser para a remoção de repintes, tendo sido preparadas maquetes representativas com tintas comerciais. A limpeza a laser advém de um estudo interdisciplinar que pretende avaliar as limitações do método utilizando parâmetros de limpeza bastante agressivos.

O uso combinado das espectroscopias de FTIR e Raman permitiu identificar os compostos das tintas modernas e, contemporaneamente, controlar o seu comportamento durante a limpeza. A microscopia óptica permitiu, por outro lado, uma avaliação da morfologia da superfície. Equipamentos portáteis do MOLAB foram também utilizados devido à importância das análises *in situ*.

A remoção dos repintes revelou-se difícil com a limpeza química, enquanto com a limpeza a laser foi mais eficaz, no entanto, provocando degradação de ligante, com formação de carbono, e alteração do branco de titânio.

O protocolo espectroscópico proposto foi considerado útil para o controlo de diferentes métodos de limpeza em pinturas de arte contemporânea.

Keywords: ligantes sintéticos, limpeza a laser, limpeza química, espectroscopia, equipamentos portáteis.

Abstract

Modern and contemporary paintings are one of today's grand challenges in conservation of cultural heritage. Particularly, these paintings have often been retouched using materials rather similar to originals, thus, compromising the reversibility of the overpainting.

In this work, FTIR and Raman spectroscopies, assisted by optical microscopy, were used to evaluate the effectiveness and harmfulness of chemical and laser cleaning methods for the removal of overpaints. Representative mock-ups prepared with commercial paint formulations were used. The laser cleaning experiment was part of an interdisciplinary study which aims the evaluation of method's limitations by using the most aggressive cleaning parameters.

The combined use of FTIR and Raman spectroscopies could identify constituent materials of modern paints, controlling their behaviour under cleaning, while optical microscopy allowed the evaluation on surface morphology. In addition, equivalent portable equipments from MOLAB were covered as a preparation for *in situ* analysis.

Several problems in the selective removal of overpaints were found with chemical cleaning. The laser cleaning showed better efficiency in removing them, although, some alterations occurred upon laser irradiation, for instance, binder degradation with carbon formation and titanium white alteration.

The proposed spectroscopic protocol was considered useful for controlling different cleaning methods in modern and contemporary paintings.

Keywords: synthetic binders, laser cleaning, chemical cleaning, spectroscopy, portable equipment.

List of Abbreviations

Er:YAG – Erbium-doped: yttrium aluminium garnet

FTIR – Fourier Transformed Infrared spectroscopy

IESL-FORTH – Foundation for Research and Technology-Hellas, Institute of Electronic Structure & Laser

ISCR – Istituto Superiore per la Conservazione ed il Restauro

MOLAB – Mobile laboratory

Nd:YAG – Neodymium-doped: yttrium aluminium garnet

OM – Optical Microscopy

PEA-MMA – Poly(ethyl acrylate-methyl methacrylate)

PVA – Poly(vinyl acetate)

SMAArt – Scientific Methodologies Applied to Archaeology and Art

T_g – Glass Transition Temperature

UV-vis-NIR – Ultraviolet-visible Reflectance/Absorbance Spectrophotometry

XRF – X Ray Fluorescence

CONTENTS

1. Introduction 8

1.1. Modern paints 8
1.2. Conservation issues on modern and contemporary paintings 11
1.3. Fundamentals of laser cleaning in conservation 11
1.4. Thesis aim 13
1.5. Optical and spectroscopic tools for cleaning control 13

2. Results and discussion 15

2.1. Mock-ups. 15
2.2. Chemical cleaning control 16
2.3. Laser cleaning control 19

3. Conclusions 28

4. References 30

APPENDICES

Appendix 1 - Materials and methods A1
Appendix 2 – Photocatalytic properties of titanium dioxide A9
Appendix 3 – General results on laser cleaning control A10
Appendix 4 – Participation on conferences A16

LIST OF FIGURES

Figure 1 – poly(ethyl acrylate) and poly(methyl methacrylate) 8

Figure 3 – Poly vinyl acetate chemical structure [4]. 9

Figure 2 – poly styrene chemical structure [4]. 9

Figure 4 – Alkyd structure containing phthalic anhydride, glycerol and linoleic acid [4]. 10

Figure 5 – Cellulose nitrate structure [6]. 11

Figure 6 – Mock-up #1 after laser cleaning. Cotton canvas on stretcher with 29 x 25 cm^2. 15

Figure 7 – OM images obtained from diverse points where the chemical cleaning method was performed. 16

Figure 8 – Reflection micro-FTIR spectra of ground layer and blue overpaint (n8 Liquitex®), for comparison with the one obtained from the area where cleaning was performed with acetone. 17

Figure 9 – Reflection micro-FTIR spectra of white overpaint (n5 Fly Color®), ... 18

Figure 10 – Reflection UV-Vis-NIR spectra obtained with the fibre-optics portable equipment, ... 19

Figure 11 – Optical microscopy images obtained from diverse points where the laser cleaning was tested. 20

Figure 13 – Fibre-optics video microscopy images obtained from the same points presented on figure 11. 21

Figure 12 – Fibre-optics video microscopy using an objective of 50x that works in contact mode with the surface of the mock-up. 21

Figure 14 – Reflection micro-FTIR spectrum of a cleaned area in n6 paint on mock-up#1 using the laser Nd:YAG 1064 nm and F = 3,02 $J \cdot cm^{-2}$, 5 pulses, compared with the white ground and canvas spectra. 22

Figure 15 – Reflection micro-FTIR spectrum of a cleaned area in n4 paint on mock-up #1 using laser Nd:YAG 355 nm (t_p = 10ns) and F = 2,06 $J \cdot cm^{-2}$, 10 pulses, compared with the n4 overpaint and white ground spectra. .. 22

Figure 16 – Reflection micro-FTIR spectrum of a cleaned area in n3 paint on mock-up#4 using the excimer KrF laser at λ = 248 nm (t_p = 30 ns, 3.06 $J \cdot cm^{-2}$, 30 pulses) compared with the n3 overpaint and white ground spectra. 23

Figure 17 – Reflection micro-FTIR spectrum of a cleaned area in n11 paint using the excimer KrF laser at λ = 248 nm (t_p = 30 ns, 3.06 $J \cdot cm^{-2}$, 30 pulses) compared with standard spectra of n11 overpaint and white ground. 24

Figure 18 – Fibre-optics FTIR spectroscopy portable equipment. Photo courtesy of SMAArt (Perugia). 24

Figure 19 – Reflection FTIR spectra, showing examples of aggressive and incomplete cleaning, by comparison with n3 overpaint, white ground and canvas standard spectra. 25

Figure 20 – Ablation in paint n4 using the Nd:YAG 355 nm laser, t_p = 10 ns, F = 2.06 $J \cdot cm^{-2}$ and 10 pulses, a) the fibre-optics portable video microscopy image from cleaned area, b) and c) optical microscopy images showing the micro black particles, d) micro-Raman spectrum (λ=532 nm) of this area with carbon assignment bands. 25

Figure 22 – Micro-Raman spectra (λ=532 nm) of phthalocyanine paint n11, performed in the remaining blue spots on the ablation areas, which showed notable fluorescence around 667 nm and 617 nm. 26

Figure 21 – Raman spectra (**λ**=532 nm) of a cleaned area on n7 paint and the standard for white ground (rutile) for comparison (normalized [0,1]) [41]. 26

Figure 23 – Fibre-optics Raman spectroscopy portable equipment. Photo courtesy of SMAArt (Perugia) 27

Figure 24 – Raman spectra (λ=785 nm) of two different ablation areas on paint n10 containing phthalocyanine blue, one successful, and other incomplete, compared with the standard spectrum of the overpaint. 27

LIST OF TABLES

Table 1 – General information about the three most important synthetic resin classes [3,4]. 10

Table 2 – Commercial paint formulations covered in the study. 15

Table 3 – General results for the cleaning experiment on mock-up #6 using solvents and chemical systems. The n6 is the considered original layer, except in its specific row, where the original layer is considered the canvas. . 19

Table 4 – General results for laser cleaning experiment on mock-up #1 and #4 using different laser systems. The n1 and the n4 are the original layers except in its specific row where the canvas is considered the original layer.27

1. Introduction

Up until the end of the nineteenth century there were mainly two typologies of easel paintings, oil and egg tempera, the first being, without doubt, the most important and diffused since Jan van Eyck (fifteenth century) [1].

However, at the beginning of the twentieth century the first synthetic materials started to emerge, as a result from the exponential growth in the paint and coatings industry. Hence, the first synthetic polymers appeared and started to be applied in paints as binding media. Not much time was needed for these materials to catch modern artists' attention. Consequently, nowadays there is a vast collection of synthetic resin based paintings, which offers new problems for painting conservation [2].

1.1. Modern paints

A synthetic resin can be present in paint formulations as a solution, that is, it is dissolved in an organic solvent, or as emulsion, which means that it is dispersed in water due to surfactants and additives [3]. Moreover, there are three important classes of synthetic resins to consider in the study of modern and contemporary paintings, namely acrylic, polyvinyl acetate, and alkyd.

Acrylic resins were the most diffused paint material in the artists' paint market. The wide variety of synthetic acrylic resins formulations is useful not only as binding medium, but also as varnishes, additives (plasticizers) which, for example, can be used in traditional painting and as restoration materials [4]. This synthetic resin appeared first in 1936 as acrylic resin for the coatings industry, but soon in 1947 the first line of artists' acrylic paints in turpentine solution was introduced by the paint maker Leonard Bocour with Sam Golden, and was commercially known by Magna®. However, it was finally in 1954 that an acrylic emulsion line for artist's use was developed, called Liquitex®, by Henry Levison from Permanent Pigments Co. After this, many other lines of artists' acrylic paints were developed by paint makers, mainly after 1964 [3].

The term "acrylic" covers a wide range of high molecular weight polymers based on acrylates and methacrylates. The only acrylic homopolymers that have the right properties to be used as acrylic solutions are the polybutyl methacrylates, namely the isomer p*n*BMA, which is used in acrylic solution paints, and p*i*BMA, more appropriate for acrylic varnishes, because of their T_g's [3]. The first was commercial available by the line Magna® and was used by important twentieth century artists, like Roy Lichenstein, Morris Louis and Kenneth Noland, although it was discontinued due the success of emulsion paints, since these offered better painting properties [3,4]. The most common synthetic resin formulations which compose emulsion paints are the copolymers composed by poly(ethyl acrylate) and poly(methyl methacrylate), which structures are showed in figure 1.

pEA pMMA

Figure 1 – poly(ethyl acrylate) and poly(methyl methacrylate) chemical structures [4].

The first acrylic emulsion grade of paints was Liquitex®, as stated before, however, other posterior grades from other producers are important to consider, as well. Examples of such are Rohm and Haas Primal® (AC-22, AC-34, AC-234, AC-634) and Rohm Plextol® B-500 [4].

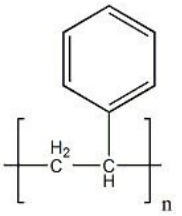

Figure 2 – poly styrene chemical structure [4].

With the aim of decreasing the overall cost of synthetic acrylic resin based paint formulations, styrene monomers are often added (structure in figure 2), shifting the final properties of the painting material, and, as a result, these are often present in low-cost household paints [3,4]. Nevertheless, it is commonly found that artists experiment these low-cost paints either by philosophy or economic reasons. Thus, the eventual analysis of these materials is important to consider in modern and contemporary paintings. An example of a commercial paint containing this compound is the Brera® paint from Maimeri, which has a terpolymer p(*n*BMA-2EHA-styrene) [3].

Polyvinyl acetate resins. The group of vinyl resins include a wide range of polymeric materials, however, in the field of plastic and coatings' industries is commonly accepted to restrict this group only to vinyl chloride polymers, vinyl acetate polymers, their copolymers, modified polymers and derivate products. The most important is the poly(vinyl acetate) resin (PVA) whose structure is shown in figure 3. The first commercial developments of PVA started in the mid 1920s as an adhesive [4]. The PVA paints are mainly waterborne emulsions. On the other hand, it usually requires the addition of plasticizers since PVA homopolymers are too brittle to form a continuous film [3].

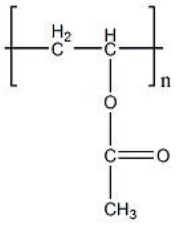

Figure 3 – Poly vinyl acetate chemical structure [4].

The most common plasticizers, sometimes in quantities up to 20% (wt%), are the phthalates, for example, the dibutyl phthalate (DBP). These external plasticizers tend to migrate to the paint surface, and therefore the paint becomes brittle and the surface more tacky and likely to have dirt pick-up [3]. In 1928 a copolymerization process was tried involving vinyl acetate and vinyl chloride, producing an emulsion paint with better properties than pure polymers or alone monomers. In the mid 1940s, vinyl acetate emulsions were introduced by DuPont Co. and others [4]. By the 1960s a copolymerization of PVA with softer monomers was accomplished, mainly with the highly branched C_9 and C_{10} vinyl esters, commercially known as vinyl versatates, or VeoVa, giving a PVA/VeoVa copolymer with improved hydrophobicity and UV resistance. However, almost every commercial PVA artist paint formulations were discontinued, except, for example, the artist grade called Flashe®, marketed by Lefranc & Bourgeois [3,5].

The PVA emulsion paints, comparing to the acrylic's, are generally considered to be slightly inferior in what respects the toughness, binding power, and resistance to weathering. On the other hand, they are less expensive and suitable for interior use [3].

Alkyd resins are oil-modified polyesters, resulting from a reaction of a polybasic acid (or polyol), a polyhydric alcohol (or poly acid) and a source of fatty acids, giving the term "alkyd" ("al" from alcohol

and “kyd” from acid). The combined product is a very flexible polymer which was introduced in the early 1930s. It had magnitude in the paint technology because of its reduced drying time and superior durability and hardness when comparing with other sources of oils. Still, alkyd resins were more famous in the household paint technology, since only Winsor & Newton produced a full colour range for artists’ use, called Griffin®, introduced in 1970. In fact, alkyd paints, as household formulations, were used by renamed artists such as Pablo Picasso and Jackson Pollock [3,4]. The most important polyols used in alkyd resins are glycerol (propan-1,2,3-triol) and pentaerythritol (2,2-bis(hydroxymethyl) 1,3-propanediol). As for the polybasic acids the most common is the dibasic acid phthalic anhydride (1,2-benzenedicarboxylic acid). The oil feature appears by the addition of a source of monobasic fatty acids, being the most common a drying oil, namely linseed and soy oils [3]. Example of an alkyd structure containing phthalic anhydride, glycerol and linoleic acid is shown in figure 4.

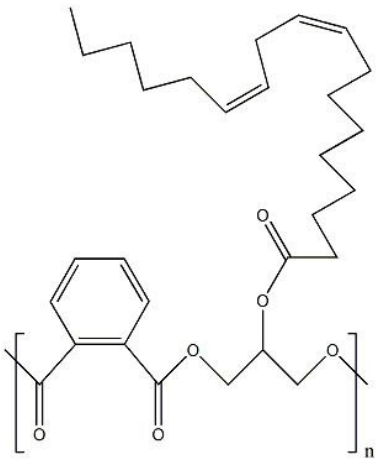

Figure 4 – Alkyd structure containing phthalic anhydride, glycerol and linoleic acid [4].

Some modifications are made to alkyd paints to improve certain properties. The most common are the addition of styrene, vinyl toluene, isocyanates, acrylic, epoxy, or silicone compounds [3]. Below a table with a summary on the three most important synthetic resin paint formulations is presented.

Table 1 – General information about the three most important synthetic resin classes [3,4].

Synthetic resin class	Chemical composition	Date of first appearance	Name of grade/ manufacturer	Artists that used it
Acrylic	**p*n*BMA** (solution)	1947	**Magna®** / Leonard Bocour and Sam Golden	Roy Lichenstein Morris Louis Kenneth Noland
	p(EA-MMA) (emulsion)	1954	**Liquitex®** / Henry Levison (Permanent Pigments Co.)	Helen Frankenthaler David Hockney Robert Motherwell Andy Warhol
PVA	**PVA** (emulsion)	1954	**Flashe®** / Lefranc & Bourgeois	Sydney Nolan Kenneth Noland Bridget Riley
	PVA/VeoVa (emulsion)	1966	**VeoVa®** / Shell Chemicals	-
Alkyd	**Polyol/polybasic acid/drying oil**	1970	**Griffin®** / Winsor & Newton	Gillian Ayres Peter Blake Patrick Caulfield Sydney Nolan Francis Picabia Pablo Picasso Jackson Pollock Pierre Soulages Frank Stella

Nitrocellulose. Other synthetic resins are also important to consider since they are included in some paint formulations that may be present in artworks, mainly in household paints. An example is nitrocellulose, which is the term applied to paints and lacquers that contain mixtures of cellulose nitrate polymer (chemical structure in figure 5) with a second resin (to improve gloss, adhesion and hardness) and plasticizers. This kind of paint only became important in the paint market after the 1920s, being

formulated as solution paint, and usually dissolved in esters, alcohols, ketones, or glycol ethers. Normally, alkyd resins are the second resin, mainly after the 1940s. As for the plasticizers, the phthalates are the most recently employed (e.g. dibutyl phthalate, dioctyl phthalate). After the 1950s, when alkyd paints started to dominate the household paint market, the nitrocellulose paints started to be sold as low-cost sprays. It was in this form that Richard Hamilton used it, and it is documented that Pollock used the solution form in his drip paintings [3].

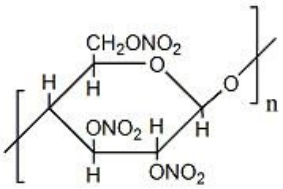

Figure 5 – Cellulose nitrate structure [6].

1.2. Conservation issues on modern and contemporary paintings

Modern and contemporary paints present new concerns in painting conservation, since they have some different properties from the traditional oil or egg tempera painting. In general, synthetic resin based paints, mainly the acrylic emulsions, are very sensible to organic solvents. This is a problem for the cleaning of artworks which contain such materials without disturbing the surface texture, colour or gloss. But, not only organic solvents cause damage to synthetic resin surfaces, also water or water-based cleaning systems can damage the paint surface, mainly because of swelling. Other main problem is the affinity for dirt pick-up when environmental conditions change, which can also be responsible for other problematic situations, for example, the irreversible mark of fingerprints and the attachment of exterior materials when they are in prolonged contact with the surface [7].

One of the most concerning problems in restoration of modern and contemporary paintings is the difficulty on the selective removal of the overpaints that are quite similar in composition to the original layers. Furthermore, it is not said that traditional restoration approaches offer a harmfulness treatment. As a matter of fact, the chemical or mechanical techniques, apart from being difficult to control, in many cases damage pigments or binders in the cleaning process. Adding to this, mechanical methods can damage the painting texture and chemicals can penetrate into the inner paint layers, ground and support, causing alterations on them. On the other hand, the actual laser cleaning method may offer a viable solution since it permits a layer by layer micro-removal [8-11]. Some experiments for the application of this method on modern and contemporary paintings have been recently tried [12-14]. However, it is still a method that has to be fine-tuned and far away to be used conventionally, due to many reasons, among which, the insufficient knowledge on laser interaction mechanisms, method expensiveness, and, the few developed diagnostic devices to provide qualitative and quantitative analysis during the laser cleaning intervention [10,15,16].

1.3. Fundamentals of laser cleaning in conservation

The emitted light from a laser is due to the energy loss of photons that are provided at one specific wavelength and one direction, being equal in this wavelength and direction. Thus, it emits a monochromatic light. For this to succeed, the majority of atoms, ions or molecules must be in the excited energy state rather than in the low-energy state (population inversion), and therefore a strong source of excitation is needed to maintain this situation, such as gaseous active materials (e.g. mixtures of noble/halogen gases in the excimer lasers) or solid active materials (e.g. the Nd^{+3} in the Yttrium Aluminium Garnet matrix) [17]. Usually, the laser ablation processes in conservation of cultural heritage aim to achieve a selective removal of material layers and, for that, conservators in general use a pulsed laser. This means that light is delivered in short energy discharges, as opposed to a

continuous wave laser. This pulsed operation allows more control, since each pulse consists of a measurable and repeatable amount of energy, which can be applied in cases with different materials and aggregation states [8,16,18,19].

Laser cleaning method is relatively recent in the area of conservation of cultural heritage, and, thus, in each case-study the project must include collaboration between conservators, conservation scientists and scientists well familiar with the physics of laser systems [18]. From 1993, the IESL-FORTH, expertise in the laser technology applied to cultural heritage, has been conducting research on laser developments for application in the cleaning of artworks. These applications comprise the laser cleaning, diagnostic analyses, imaging and authentication techniques. In 1995, for the first time a workshop on lasers applied to conservation was organized, named LACONA (Lasers in the Conservation of Artworks), which continues nowadays as an international biannual conference. In recognition to that, conservators became more familiar to laser technology and several research groups have been formed to develop its application in artworks, as is the example of the European research project “advanced workstation for controlled laser cleaning of artworks” [8,9,20].

Laser cleaning of paintings is very controversial, mainly because many studies are still being developed on the short and long term irradiation effects on pigments and binding media, which can be thermal, photochemical or photomechanical [9,21-23]. Thermal effects depend on the thermal diffusivity parameters of the material, the laser system’s pulse length (t_p) and wavelength. Photochemical alterations are expected to be the main source of cleaning procedure side effects, mainly because of the radicals and ions produced during the irradiation, which can react and form photo-oxidation products. As for the photomechanical effects, it has been demonstrated the development of stress waves, which can be significant, especially when high laser fluences are employed [24]. There are mainly three kinds of laser systems that are currently being applied for the conservation of cultural heritage: excimer, Nd:YAG and Er:YAG lasers.

Excimer lasers (short name for excited dimmer) are based on rare gas-halide mixtures, emitting mainly in the UV region: ArF λ = 193 nm; KrF λ = 248 nm; XeCl λ = 308 nm; XeF λ = 351 nm. These laser systems are useful for treating paintings since the materials traditionally employed in paintings (varnishes and overpaints) absorb strongly in the UV, and therefore cause minimal light penetration to inner layers, although it is a more energetic regime. Because this effect depends on the nature and specific properties of the material substrates, it requires the optimization of laser parameters (energy density (F), pulse length (t_p), number of pulses) to the particular needs of the application [9,14,18,19,24,25].

Nd:YAG lasers have been studied since the 1970s, firstly for the cleaning of stone surfaces. It is a neodymium-doped: yttrium aluminium garnet (Nd: $Y_3Al_5O_{12}$) emitting generally in the near infrared region (NIR) at λ = 1064 nm (ω). However, it can also emit other radiations by multiplying the fundamental frequency: λ = 532 nm (2ω); λ = 355 nm (3ω); λ = 266 nm (4ω); and λ = 213 nm (5ω). It has been explored, only recently, in what concerns its application on the cleaning of paintings, because it offers better results in breaking bonds of inorganic materials. However, it must be carefully controlled because of its deep irradiation penetration [9,14,19,26].

Er:YAG lasers are also applied for the cleaning of artworks, even if only more recently. It is an acronym for erbiumdoped: yttrium-aluminium-garnet (Er: $Y_3Al_5O_{12}$). It emits radiation at 2940 nm, which is high-absorbed by the OH bonds, permitting very superficial ablation depths. However, in

cases where the materials are not rich in OH bonds, hydroxylated liquids can be added to control the radiation penetration and limit the heat effect [9,27].

An important aspect is the ablation threshold, the point at which absorbed laser energy is sufficient to break the bonds between molecules of a material. Hence, the careful determination of the laser fluence values at which substrate damage threshold occurs, is important for a safe cleaning [10].

1.4. Thesis aim

For good practice in the conservation of modern and contemporary artworks the characterisation of constituting materials is necessary in order to apply correct methodologies that can contribute to the painting's longevity. Apart from such, information concerning the material composition can give important information to art historians, for instance, on artist's creative process or about the originality in employing new materials not yet available in artists' market. Even if today's ethical values and international recommendations defend a much more preservation/conservation practice than a curative one, some critical cases must be re-thought, e.g. a monochromatic painting with posterior overpaints which interfere with the original colour homogeneity intended by the artist, or a painting in direct contact with storage materials (e.g. polyethylene) that can easily attach to the painted surface. In both cases the removal of non original materials may be considered. However, taking into account the difficulty in removing this kind of layers in modern and contemporary paintings, a study has necessarily to be overcome by scientific investigative assistance.

Considering the statements above, the aim of this thesis was to apply diverse spectroscopic tools for the qualitative analysis of the elemental and chemical composition of painted surfaces, in order to evaluate and control different chemical cleanings, whilst, contemporarily assessing the laser cleaning of modern and contemporary paintings. Since the cleaning of this kind of artworks is still a very delicate subject considered border-line between an efficient and a too evasive cleaning, this thesis aims to offer a spectroscopic protocol that permits a liable evaluation on the effectiveness and harmfulness of the cleaning method applied.

One of the aims of this work was also to evaluate the results equivalence between portable equipments from MOLAB[1] and the ones obtained from bench equipments. This is important since the latter are more adequate for mock-ups analysis in laboratory, while portable equipments are important for *in situ* analysis in case studies.

1.5. Optical and spectroscopic tools for cleaning control

The spectroscopic tools that were considered relevant were FTIR and Raman spectroscopies. Other efficient analytic techniques have been proposed by authors for the characterisation of modern paints [3,7], e.g., Pyrolysis-Gas Chromatography-Mass Spectrometry (Py-GC-MS), Pyrolysis-Gas Chromatography (Py-GC), and Direct Temperature-Resolved Mass Spectrometry (DTMS), which are destructive techniques and therefore not appropriate for controlling cleaning procedures. FTIR and Raman spectroscopies are not only non-invasive techniques but also suitable to be applied *in situ*, due to the fibre-optics portable equipments.

- FTIR spectroscopy. FTIR spectroscopy is a technique that allows the identification of molecular bonds in a material by their resonance frequencies. The group frequency region (or functional group)

[1] MOLAB is a mobile laboratory with a "transnational access" composed by a unique collection of portable equipments, suitable for *in-situ* non-destructive studies and diagnosis. It belongs to CHARISMA project (http://www.charismaproject.eu/transnational-access/molab.aspx)

exists from 4000 to 1300 cm^{-1}, where there is information about the chemical classes present in the sample, while from 1300 to 500 cm^{-1}, is the called “fingerprint region”. Even if more difficult to interpret, it contains specific bands for each compound, which can be matched with standards in databases. For this reason, FTIR analytical method is ideal for painting medium characterisation. However, when dealing with the characterisation of modern artists’ paints, the interpretation becomes more complex, because relevant library of known standards are still being built. Besides that, paint formulations have different components (binder, pigment, extender, additives) and sometimes one particular element may dominate the entire FTIR spectrum, masking the other components characteristic bands [3].

Of relevance in cultural heritage analyses is the reflection FTIR spectroscopy, since it permits a non contact analysis and no sample preparation. However, each spectrum obtained depends on the area analysed morphology and its optical properties, giving large distortions in the spectra, both in band shape and position [4,10,28-33]. There are three modes of external reflection measurements in spectroscopy: transmission-reflection (or transflection), specular reflection and diffuse reflection. Reflection FTIR spectroscopy generally collects both specular and diffuse reflection with a ratio that depends in majority on the surface roughness [4,34]. Specular reflection is observed when the material has a very smooth and flat surface which reflects the incident irradiation. Diffuse reflection, on the contrary, results from materials with rather rough surfaces, which scatter irradiation over a wide range of angles [4].

Specular reflection is based on Fresnel’s equations, depending in both absorption coefficient (k) and refractive index (n) [34]. Fresnel reflection gives quite distorted spectra, depending on the band strength. One example is the *reststrahlen* effect, often seen in minerals, which means a reflectance maximum occurring for those fundamental bands that show $k >> n$ corresponding to total inverted bands shape. For weaker bands, the dispersion of n origins bands in a first derivative shape of a normal absorption or reflection band [4,34].

Diffuse reflection is governed by the Kubelka–Munk model, depending on the parameters k and s, which are the absorption and scattering coefficients, respectively. The spectrum obtained from diffuse reflection is not related to peak intensity and composition. In fact, weak absorption bands show an intensity increase in respect to stronger absorption bands. Hence, it is usually observed that relative intensities of overtones and combination bands are larger in reflection spectra than in traditional transmission ones [4,34].

With the stated above one can understand the difficulty in interpreting reflection FTIR spectra from paintings, due to the co-existence of specular and diffuse components of reflection in the surface, which cannot be resolved individually using the mathematical algorithms above, and therefore, the spectra interpretation must be accomplished with such distortions [4].

- Raman spectroscopy. Raman spectroscopy is a light scattering technique and its spectra can provide information on molecular structures, which can be used to identify both organic and inorganic materials, making it an ideal analytical method for pigment analysis, along with its sensitivity and reliability. One of the disadvantages relies on the broadband fluorescence, which may overlay Raman signals [10,31].

The optical microscopy (OM) was chosen for the surface morphology analysis before and after cleaning. The Scanning electron microscopy (SEM) and Atomic force microscopy (AFM) have also been used by authors to document film coalescence and morphology [4,10,18]. However, SEM does

not have yet equivalent portable equipment and the one of AFM is still too much sensible to exterior factors to be used routinely *in situ*. A portable fibre-optics video microscopy was preferred as the OM equivalent equipment, since it is easy to use and it gives useful information on morphology and material distribution.

Other spectroscopic techniques are being used for the cleaning control such as laser-induced breakdown spectroscopy (LIBS) and laser-induced fluorescence (LIF), which, however, are not available at the MOLAB [13,22,35,36].

2. Results and discussion

2.1. Mock-ups.

It was intended that the mock-ups used for the development of this thesis would be representative of the materials that can usually be found in modern and contemporary paintings. Therefore, the emphasis was made on the diversity of synthetic binding media, since in this area much research is still in development for the adequate chemical characterisation of synthetic binder formulations in modern paints [3,4]. Thus, the study involved, mainly, the three classes of synthetic resins: acrylic, polyvinyl acetate, and alkyd. A mixture between nitrocellulose and alkyd was also covered. Different pigments were studied, which together with the binding media give the ready-mixed commercial paint formulations used, presented in table 2 (for more information on the materials see appendix 1, page A1-A5). Figure 6 shows one of the prepared mock-ups.

Figure 6 – Mock-up #1 after laser cleaning. Cotton canvas on stretcher with 29 x 25 cm^2.

Table 2 – Commercial paint formulations covered in the study.

	White paints	Blue paints
Artist's use	**n1 – Polycolor®** *PVA/VeoVa,* Titanium white **n2 – Liquitex®** *PEA-MMA*, Titanium white **n3 – Griffin®** *Alkyd,* Titanium white	**n7 – Polycolor®** *PVA/VeoVa,* Ultramarine blue **n8 – Liquitex®** *PEA-MMA,* Ultramarine blue **n9 – Griffin®** *Alkyd* Ultramarine blue
Household	**n4 – Boero®** *Alkyd,* Titanium white **n5 – Fly color®** *Styrene-acrylic spray,* Titanium white **n6 – Belton Molotow®** *Nitrocellulose-alkyd spray,* Titanium white with iron component	**n10 – Boero®** *Alkyd,* phthalocyanine blue **n11 – Fly color®** *Styrene-acrylic spray,* phthalocyanine blue and dioxazine violet **n12 – Belton Molotow®** *Nitrocellulose-alkyd spray,* Dioxazine violet

Furthermore, the mock-ups offer the possibility to test the difficulty on removing overpaints rather similar to the original layer, either by composition or colour. For instance, the white paints over the white ground represent what most probably the restorer will have to face in an overpainted artwork.

Towards a better understanding, the organisation of the results will be presented taking as base first the experience of the chemical cleaning and then the one with laser cleaning. In the chemical cleaning chapter only optical microscopy and FTIR spectroscopy were covered. As for the laser cleaning, since it was considered of most importance in the development of the overall work, a more developed study was elaborated: optical microscopy, FTIR and Raman spectroscopies were used, as

well as the equivalent fibre-optics portable equipment. In the FTIR spectroscopy, analyses were made using the transmission mode (preparing KBr pellets), for paint materials characterisation, and in reflection mode, both in bench and portable equipment, for the cleaning control.

2.2. Chemical cleaning control

For this experiment eight solvents (covering ketones, alcohols, aromatics, esters and hydrocarbons) and chemical systems were chosen. The mock-up prepared for this chapter has a white ground (considered the original layer) prepared with paint n6 Belton®. The cleaning experimental work was performed by an experienced restorer in the conservation of modern and contemporary paintings.

In a first simple observation by naked eye it was possible to verify that the blue paints were more easily removed (more the ultramarine blue paints than the phthalocyanine or dioxazine paints). It was also confirmed what was already stated in the introduction about the action of solvents or water-based solutions in modern paints. In fact, it was observed that in some cases alterations on the surface occurred significantly, such as change of gloss, damage in inner layers, incorporation of overpaint into original layer, etc.

- Optical Microscopy (OM). The images obtained with optical microscopy (figure 7) confirmed some of the chemical cleaning problems explained previously.

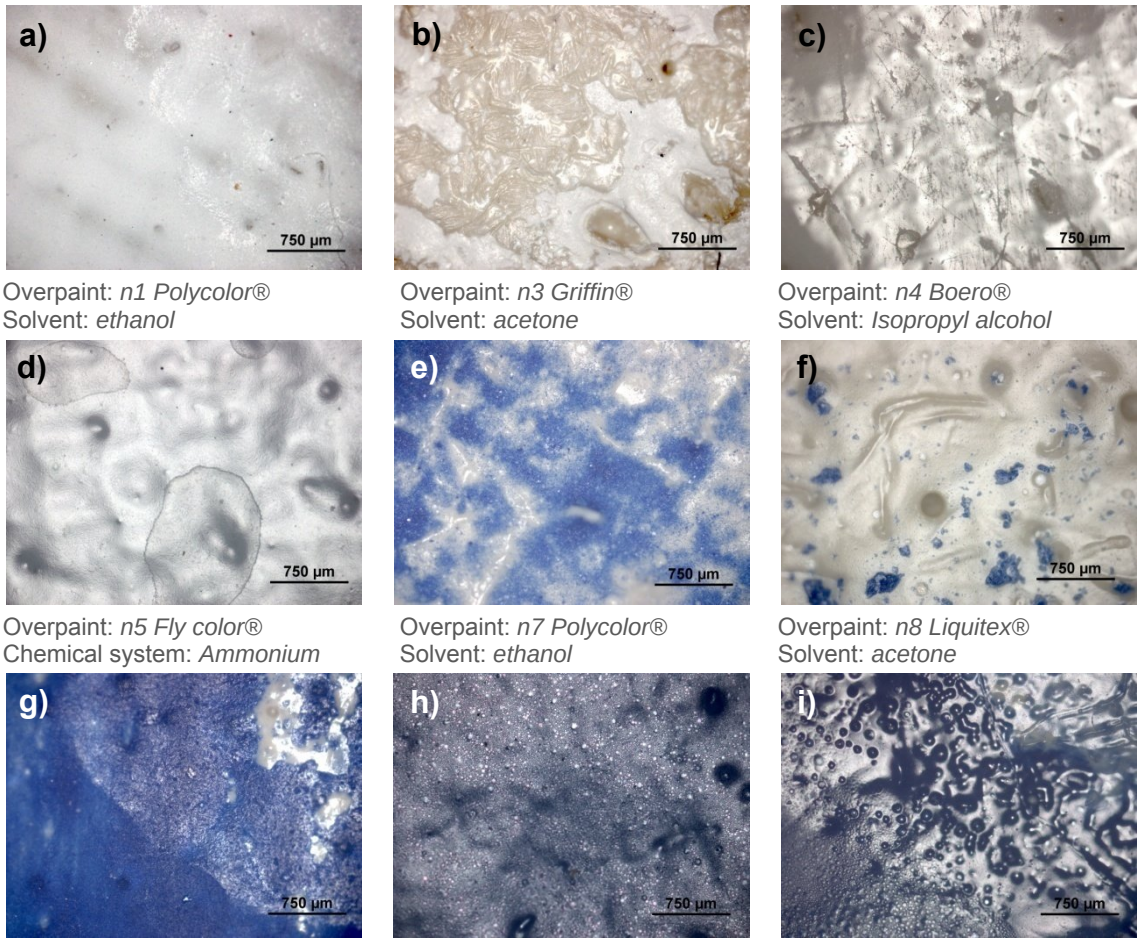

Figure 7 – OM images obtained from diverse points where the chemical cleaning method was performed.

For example in figure 7a) and g) it is possible to see an alteration on the surface gloss, which also indicates the exact area where the solvent was applied. Furthermore, this effect was seen in all blue paints containing ultramarine blue and cleaned with acetone. Other situations could be found, as for example the cleaning heterogeneity - figure 7b), e) and f) -, over cleaning - figure 7b) -, mechanical damage to the surface without removing the overpaint, possibly caused by the cotton swab - figure 7c) -, deposit marks from the left over solvent -figure 7d) -, swelling effect - figure 7h) -, and a mixture caused by the solvent, between the overpaint and the original layer - figure 7i) -, which are same binder based (nitrocellulose and alkyd), and therefore, it was already expected to occur.

- FTIR spectroscopy. With the aim of assessing the chemical cleaning effectiveness and harmfulness a FTIR analysis was performed taking into account the binder behaviour under the cleaning in what respects: bands intensity, shifting of band position, relative increasing/decreasing of bands, and changes between derivative and positive maximum bands; comparing spectra with the standard ones obtained from the white ground (the considered original layer) and the overpaints [37,38].

As mentioned in the introduction, reflection spectroscopy has some practical implications in spectra interpretation. In this work, the mock-ups prepared have a quite rough surface and, therefore, rather being a disadvantage, it is an opportunity to prepare for the experience of interpreting reflection spectra when analysing an artwork *in situ*. For instance, in the example given in figure 8 it is possible to observe that the spectrum of the blue overpaint (ultramarine blue) has the silicate in-plane vibration assignment band in a *reststrahlen* inversion at about 1006 cm^{-1}. The spectrum collected in the remaining blue overpaint of the cleaned area shows alterations in band shape. In fact, band has assumed a first derivative, possibly due to alteration to the optical properties of the surface or due to other bands interferences from ground layer.

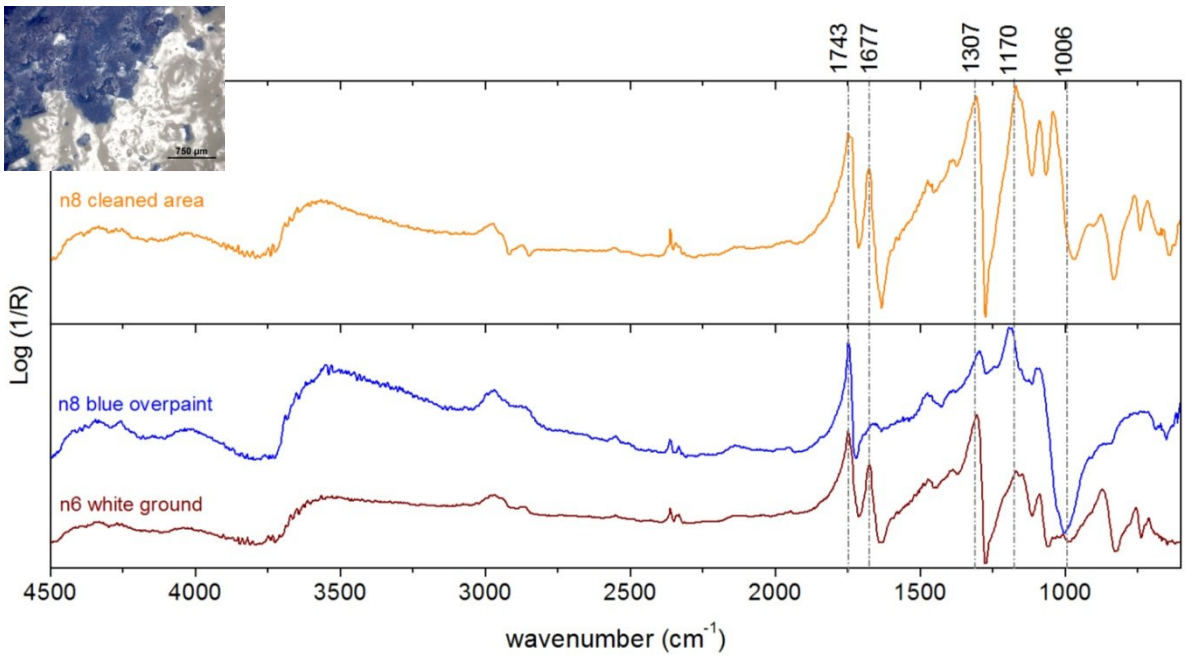

Figure 8 – Reflection micro-FTIR spectra of ground layer and blue overpaint (n8 Liquitex®), for comparison with the one obtained from the area where cleaning was performed with acetone.

The cleaning was not efficient because it could not completely remove the blue overpaint, showed by the ultramarine blue silicate presence in the spectrum of the cleaned area. Adding to this, the OM showed that cleaning was heterogeneous, leaving several residuals of blue overpaint.

Taking into account the analysis made on the paints containing phthalocyanine or dioxazine pigments, it had been observed that the binder is removed first than these organic dyes. In fact, in the spectra the bands associated to them become more clear and sharp. In addition, it was observed by OM that in the cleaned areas with acetone the blue pigment incorporated into the ground paint matrix.

About the white paints, another example of a partial cleaning is given in figure 9. In this example, xylene was the solvent used, which has an aromatic structure. With the principal “like dissolves like”, it is possible that this solvent had more interaction with the aromatic moiety styrene from the styrene-acrylic copolymer paint. In fact, a relative decreasing of the assignment bands of the aromatic C-H out-of-plane bending is visible (746 cm^{-1} and 698 cm^{-1}). Also, the aromatic ring breathing area shows a slight relative decreasing. The same effect is visible in the corresponding blue paint (n11 Fly Color®).

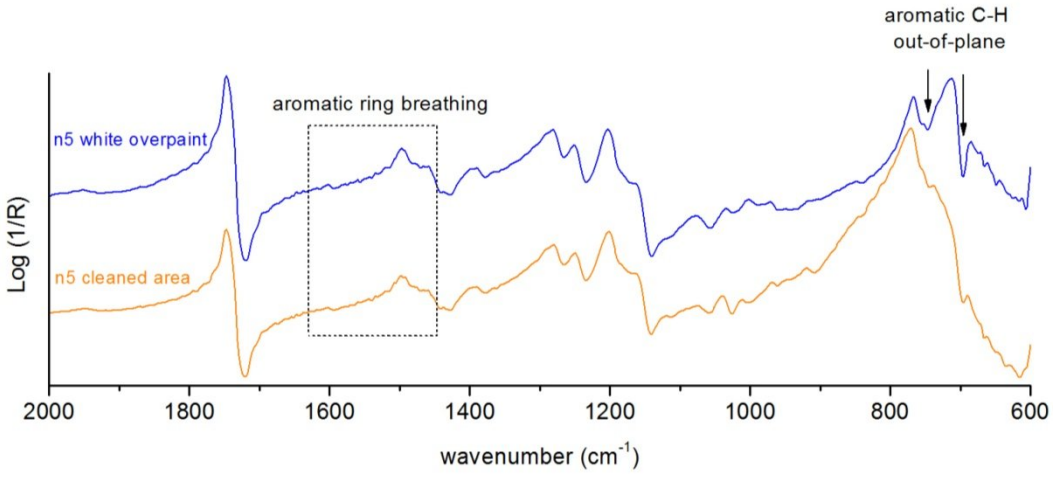

Figure 9 – Reflection micro-FTIR spectra of white overpaint (n5 Fly Color®), and of the correspondent cleaned area using xylene.

In general, the efficiency in removing white paints was lower, which can be explain by the fact that the restorer had more difficulty in perceiving if it could go further or not with the cleaning.

Further below, a table is presented with the compiled results on the chemical cleaning effectiveness and harmfulness, obtained by interpretation of the results from OM and FTIR spectroscopy (table 3).

By analysing the table, it is possible to highlight the following. Deionized water was not able to remove any overpaint, although it could interfere with the surface causing it to swell. Also ammonium and petroleum ether were not efficient cleaning agents. On the other hand, acetone was the solvent with better efficiency in removing overpaints, although, with a strong action in dissolving paint layers, sometimes reaching canvas. This can be easily explained by the fact it belong to the ketones group (RC(=O)R') and therefore can easily interact with oxygen and break the esters bonds that compose the majority of synthetic resins studied (RC(=O)OR’). Furthermore, it was the only solvent that could remove the paints n6 and n12, both nitrocellulose and alkyd based. The ethyl lactate also showed acceptable results regarding cleaning effectiveness, mainly in the PVA and acrylic paints, which can be explained by the fact it belongs to the esters functional group. Ethanol, isopropyl alcohol, and xylene solvents revealed medium efficient results (partial cleanings).

Table 3 – General results for the cleaning experiment on mock-up #6 using solvents and chemical systems. The n6 is the considered original layer, except in its specific row, where the original layer is considered the canvas.

Solvent / Paint	Deionized water	Acetone	Ethanol	Isopropyl alcohol	Xylene	Petroleum ether 80-100°C	Ethyl lactate	Ammonium
n1 –Polycolor®	- *	+++	- *	+	++	-	++	-
n2 – Liquitex®	-	++	- *	-	++ *	-	+++	-
n3 – Griffin®	- *	++ !	+ *	+ *	+ *	-	+	-
n4 – Boero®	-	+++ *!	++ *	- *	- *	-	- *	- *
n5 – Fly color®	-	+ *	- *	-	+ *	-	+	- *
n6 – Belton®	- *	++	+	-	-	-	-	-
n7 – Polycolor®	- *	+++ *	++	++	++	- *	++ *	-
n8 – Liquitex®	- *	+++ *	++ *	++	++	- *	+++ *	+ *
n9 – Griffin®	- *	+++ *	++	+ *	+ *	- *	++ *	- *
n10 – Boero®	-	+++ *!	++	++ *	+	-	++	-
n11 – Fly color®	- *	+++ *!	- *	- *	- *	-	+ *	- *
n12 – Belton®	- *	+++ !	- *	- *	- *	- *	- *	- *

(-) no removal; (+) minor removal; (++) significant removal but with several overpaint residuals; (+++) total removal; (*) damage/alteration to the overpaint; (!) damage/alteration to the ground layer.

2.3. Laser cleaning control

Preliminary laser cleaning tests were performed mainly on a spot basis, in order to define the optimum parameters for efficient and safe overpaint removal and to establish the limitations of this method, by using the most aggressive cleaning parameters.

Hence, with that proposal four mock-ups were used, each one with a different white ground, namely, mock-up#1 – n1 Polycolor®; mock-up#2 – n2 Liquitex®; mock-up#3 – n3 Griffin®; mock-up#4 – n4 Boero®. However, only the mock-ups #1 e #4 were analysed in this work, since they covered all laser systems in study: mock-up #1 – laser Nd:YAG at λ = 1064 nm (t_p= 10 ns), λ = 532 nm (t_p= 10 ns) and λ = 355 nm (t_p= 10 ns and 150 ps) and excimer KrF at λ = 248 nm (t_p= 30 ns); mock-up #4 – Nd:YAG laser at λ = 355 nm (t_p= 150 ps) and excimer KrF laser at λ = 248 nm (t_p= 30 ns). To assist the interpretation of the results on pigment alteration upon laser irradiation, reflection UV-Vis-NIR spectra were obtained (figure 10), showing that titanium dioxide (TiO_2) absorbs strongly in the UV zone. The n6 white paint, despite containing an iron component, which gives an ivory colour, has still a big absorption under 400 nm. As for blue paints, the ultramarine blue spectra show an absorption band centred at 590 nm, the phthalocyanine centred at 640 nm, and the dioxazine centred at 620 nm.

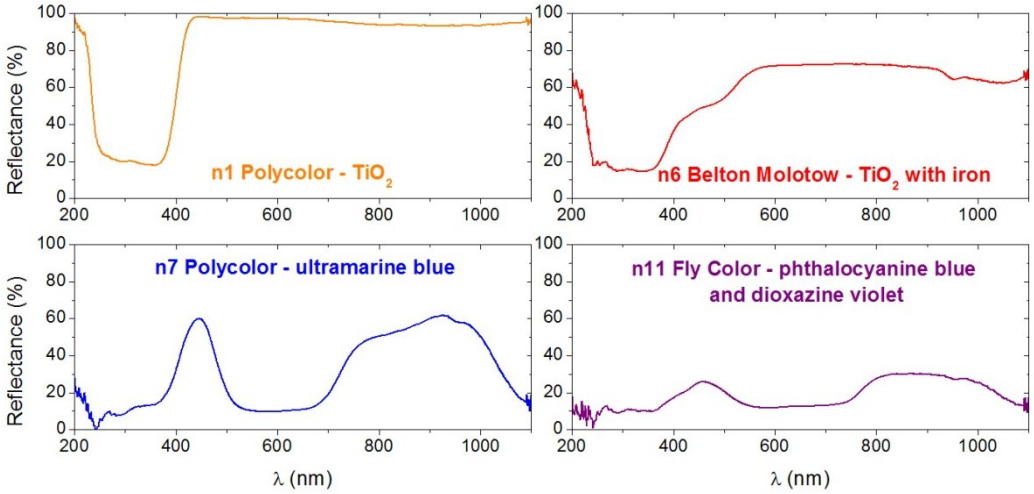

Figure 10 – Reflection UV-Vis-NIR spectra obtained with the fibre-optics portable equipment, from four different commercial paints.

In all four canvases, the laser irradiation revealed in most cases a greyish discoloration in the white paints and a black-halo around some of their ablation areas. In what concerns the irradiation effect on blue paints, they seem to have been more easily removed and there is no visible alteration phase around their ablation areas.

The discoloration in paints is always a big problem in laser irradiation and in this specific case can be due to two situations: pigment or binder degradation/alteration. The greyish discoloration of paints containing titanium white is not new. In fact, authors have already observed this effect [21,39] defending that it can be caused by a chemical decomposition of the metal oxides or by physical effects (increase of particle size).

- Optical Microscopy. *O*ptical microscopy observations clarified about cleaning homogeneity of the cleaned areas; discoloration on the white paints; presence of black-halos around ablation areas; aggressive cleanings, etc. Some examples are given in figure 11.

In fact, in figure 11a) and d) it is perfectly visible that the cleaning was aggressive, with canvas exposure. Further, several residuals of the blue overpaint on the d) were also observed, which cannot be a redeposition of the ablated material, since it was not observed around the crater, and it would have a darker appearance. The most reasonable is that it is related to the inhomogeneities of the laser beam. This last feature can also be correlated to the image from figure 11b) and f), all using different laser systems.

The aggressive cleaning seen with the laser Nd:YAG 1064 nm is possibly related to the wavelength, and thus, has to be still carefully studied before thinking its application on painted artworks.

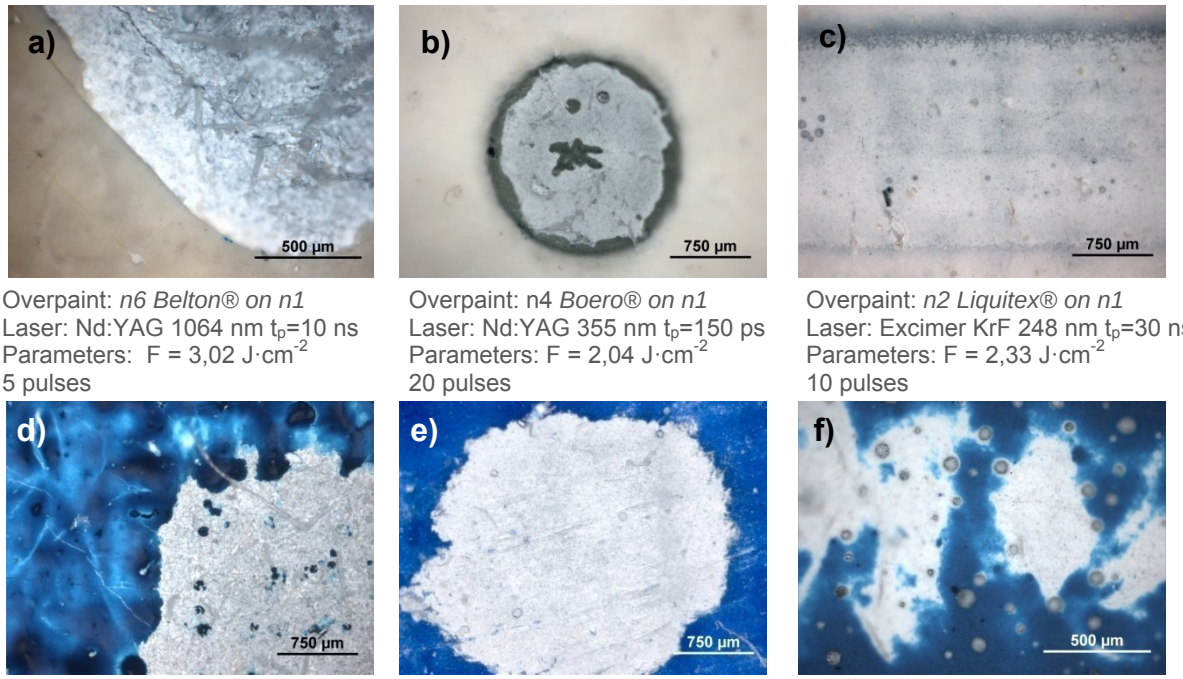

Overpaint: *n6 Belton® on n1*
Laser: Nd:YAG 1064 nm t_p=10 ns
Parameters: F = 3,02 J·cm^{-2}
5 pulses

Overpaint: n4 *Boero® on n1*
Laser: Nd:YAG 355 nm t_p=150 ps
Parameters: F = 2,04 J·cm^{-2}
20 pulses

Overpaint: *n2 Liquitex® on n1*
Laser: Excimer KrF 248 nm t_p=30 ns
Parameters: F = 2,33 J·cm^{-2}
10 pulses

Overpaint: *n10 Boero® on n1*
Laser: Nd:YAG 1064 nm t_p=10 ns
Parameters: F = 3,02 J·cm^{-2}
3 pulses

Overpaint: *n9 Griffin® on n1*
Laser: Nd:YAG 355 nm t_p=10 ns
Parameters: F = 2,06 J·cm^{-2}
10 pulses

Overpaint: *n11 Fly Color® on n1*
Laser: Excimer KrF 248 nm t_p=30 ns
Parameters: F = 3,06 J·cm^{-2}
50 pulses

Figure 11 – Optical microscopy images obtained from diverse points where the laser cleaning was tested.

In figure 11b) a black halo around the crater of the ablation area is visible, which can be explained by the fact that laser energy in the border is lower than at the centre, and thus, does not have enough energy to remove the material, leaving it damaged. In this figure, the already referred greyish discoloration is also visible. Furthermore, with a bigger magnification it is possible to observe presence of various micro black particles that can be responsible for the grey tone. On the contrary, in figure 11c) and e) examples are shown of what could be an approximation of a successful cleaning, i.e. with removal of overpaint and minimal damage to inner layers.

In general, in a first observation, the lasers in the UV regime (excimer KrF laser at λ = 248 nm and Nd:YAG laser at λ = 355 nm) have given the best results. On the other hand, Nd:YAG at λ = 532 nm showed several defects on the beam profile. In fact, the few examples where the overpaint removal was complete a black halo on the limits of the ablation area was visible, although only on the white paints. Also the excimer KrF (248 nm) and the Nd:YAG (355 nm, t_p = 150 ps) showed some defects in the beam profile.

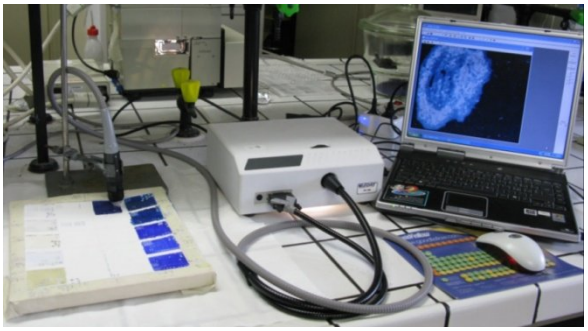

Figure 12 – Fibre-optics video microscopy using an objective of 50x that works in contact mode with the surface of the mock-up.

The equivalent portable equipment (figure 12) allowed obtain very similar images to the ones acquired with OM, as it can be seen in figure 13. In fact, even if the objective magnification permitted by this equipment is lower than the one from OM, it is possible to make the same observations made before by analysing the images below, and therefore this portable equipment proves that it has the reliability to be used *in situ* for cleaning control.

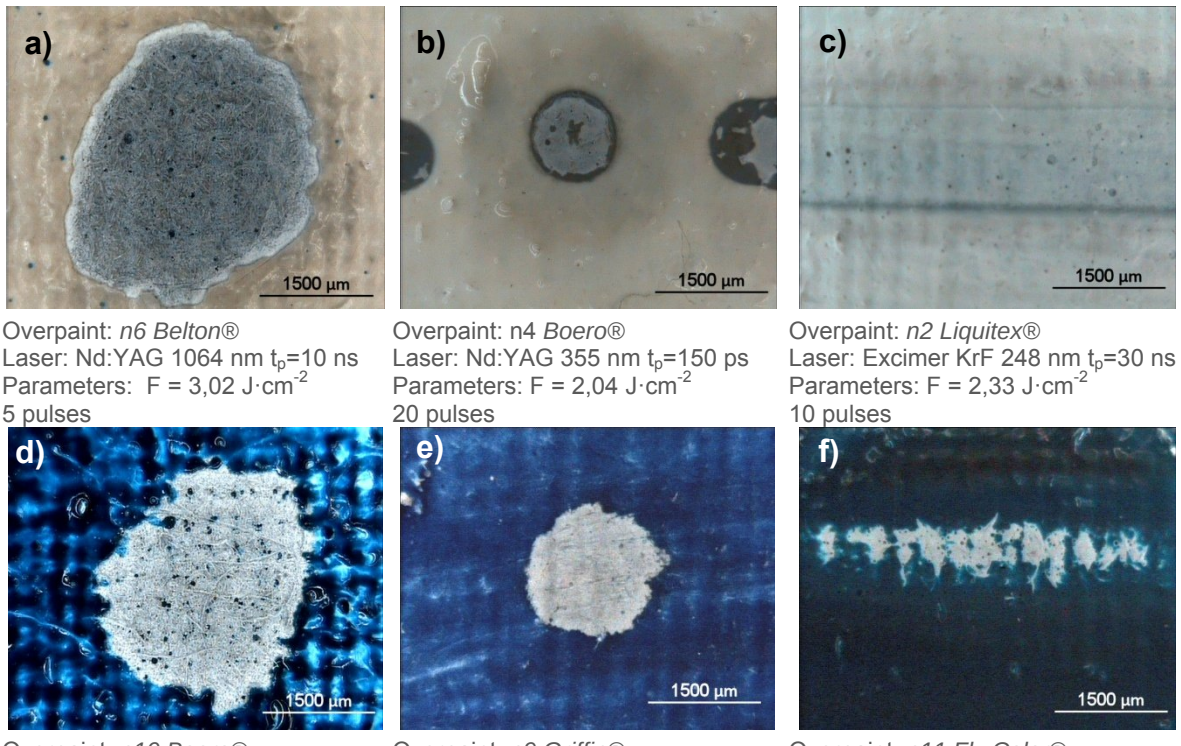

Overpaint: *n6 Belton®*
Laser: Nd:YAG 1064 nm t_p=10 ns
Parameters: F = 3,02 J·cm^{-2}
5 pulses

Overpaint: n4 *Boero®*
Laser: Nd:YAG 355 nm t_p=150 ps
Parameters: F = 2,04 J·cm^{-2}
20 pulses

Overpaint: *n2 Liquitex®*
Laser: Excimer KrF 248 nm t_p=30 ns
Parameters: F = 2,33 J·cm^{-2}
10 pulses

Overpaint: *n10 Boero®*
Laser: Nd:YAG 1064 nm t_p=10 ns
Parameters: F = 3,02 J·cm^{-2}
3 pulses

Overpaint: *n9 Griffin®*
Laser: Nd:YAG 355 nm t_p=10 ns
Parameters: F = 2,06 J·cm^{-2}
10 pulses

Overpaint: *n11 Fly Color®*
Laser: Excimer KrF 248 nm t_p=30 ns
Parameters: F = 3,06 J·cm^{-2}
50 pulses

Figure 13 – Fibre-optics video microscopy images obtained from the same points presented on figure 11.

- FTIR spectroscopy. This spectroscopic tool permitted to evaluate the cleaning effectiveness in a molecular level, especially in what concerns the binder behaviour under laser cleaning.

In what concerns first the analyses made on mock-up #1, it was confirmed that, in the majority of cases, cleaning with the Nd:YAG laser at λ = 1064 nm was injurious to the original paint, because when the laser could eliminate completely the overpaint, in almost every cases was damaging the ground layer and therefore the spectra show also bands corresponding to the canvas (see figure 14).

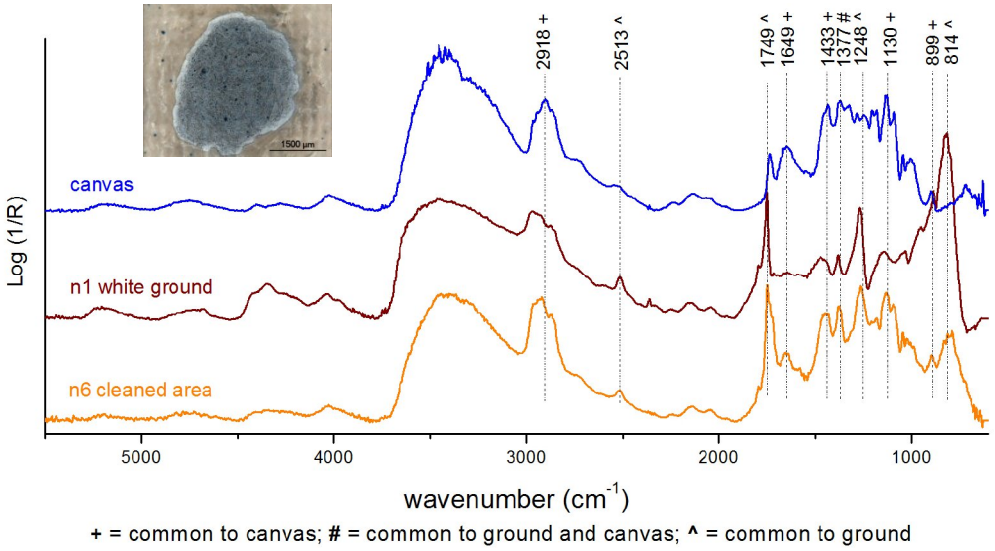

Figure 14 – Reflection micro-FTIR spectrum of a cleaned area in n6 paint on mock-up#1 using the laser Nd:YAG 1064 nm and F = 3,02 J·cm^{-2}, 5 pulses, compared with the white ground and canvas spectra.

In fact, the spectrum from the ablated area is very similar to the one from canvas. However, some signals assigned to the ground are still visible, namely the bands at 1248 cm^{-1} (first derivative shape) and 1749 cm^{-1}, corresponding to the C-O-C symmetric stretching and C=O stretching of PVA, respectively [4].

In general, the laser irradiation with the Nd:YAG 532 nm offered less cleaning effectiveness because, in most cases, it did not reached the original layer, and when it reached there were still several residuals from the overpaint.

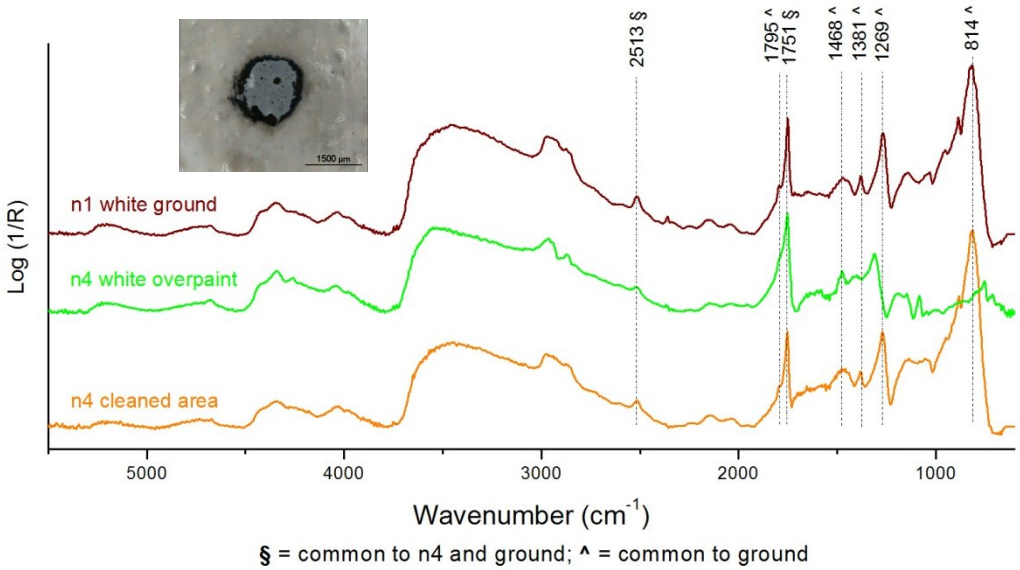

Figure 15 – Reflection micro-FTIR spectrum of a cleaned area in n4 paint on mock-up #1 using laser Nd:YAG 355 nm (t_p = 10ns) and F = 2,06 J·cm^{-2}, 10 pulses, compared with the n4 overpaint and white ground spectra.

On the contrary, the results obtained with the laser Nd:YAG 355 nm, were the most satisfactory in removing overpaints, i.e. analysing the different spectra, it is possible to observe cleaning homogeneity and a progressive micro layer-by-layer removal. Adding to this, spectra of the most efficient cleaned areas showed the best similarity to the spectrum of white ground layer. An example of this is given in figure 15. Even if OM shows white ground discoloration, FTIR analysis demonstrated that the overpaint was completely removed, considering the difficulty in assessing visually an efficient removal of a white overpaint over a white ground. The white discoloration will be explained further by Raman spectroscopy.

The analysis made on the cleaned areas with the excimer KrF laser (λ = 248 nm) showed, as well, satisfactory results, even if problems like the darkish halo around ablated areas, discoloration of the white paints, and inhomogeneities of the laser beam, were still present.

About the analyses made on the mock-up #4, it was observed that the resulting spectra were quite "noisy", due to the rougher surface of this mock-up, making it more difficult to interpret. This is one of the reasons why it is essential the acquisition of standard spectra of overpaints and the original layers (when possible) very near where the cleaning experiment is being tested.

The following example of ablation with the excimer KrF 248 nm (

figure **16**) is an incomplete cleaning, even if the OM image suggests an efficient overpaint removal.

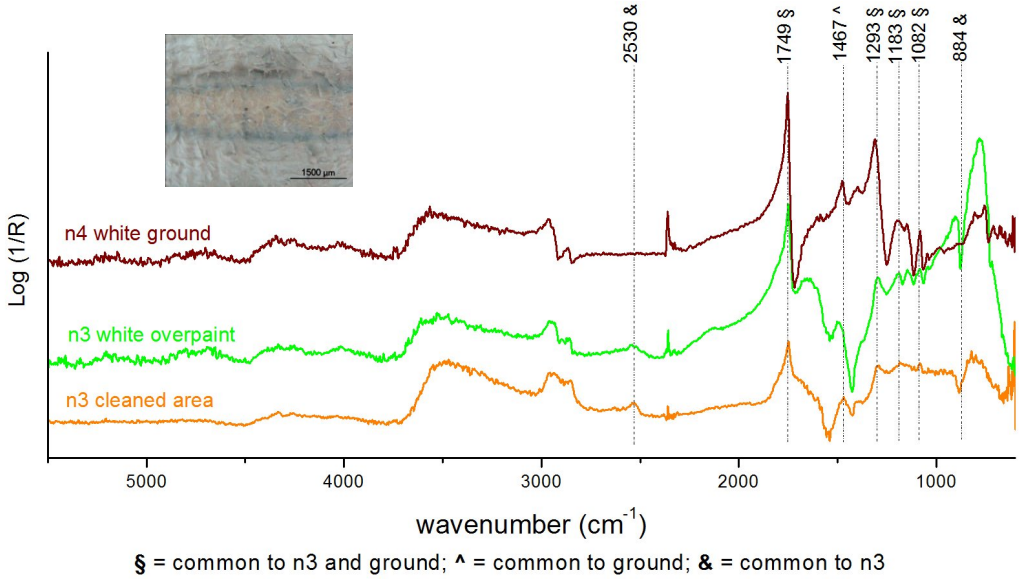

§ = common to n3 and ground; **^** = common to ground; **&** = common to n3

Figure 16 – Reflection micro-FTIR spectrum of a cleaned area in n3 paint on mock-up#4 using the excimer KrF laser at λ = 248 nm (t_p = 30 ns, 3.06 J·cm^{-2}, 30 pulses) compared with the n3 overpaint and white ground spectra.

Although paints n3 and n4 are both alkyd based, the overall aspect of the spectra is different enough to affirm that the overpaint removal was not complete. For example the bands at 2530 cm^{-1} and 884 cm^{-1} are definitely assigned to the n3 overpaint, which contains calcite, while the one at 1467 cm^{-1} is assigned to the white ground.

On the contrary, in figure 17, an example of a successful cleaning is presented. In fact, the spectrum of the ablated area is very similar to the one from the white ground (see assigned bands), even the aromatic ring breathing doublet bands (with few intensity) characteristic of alkyds at 1603 cm^{-1} and 1586 cm^{-1} [4] are visible.

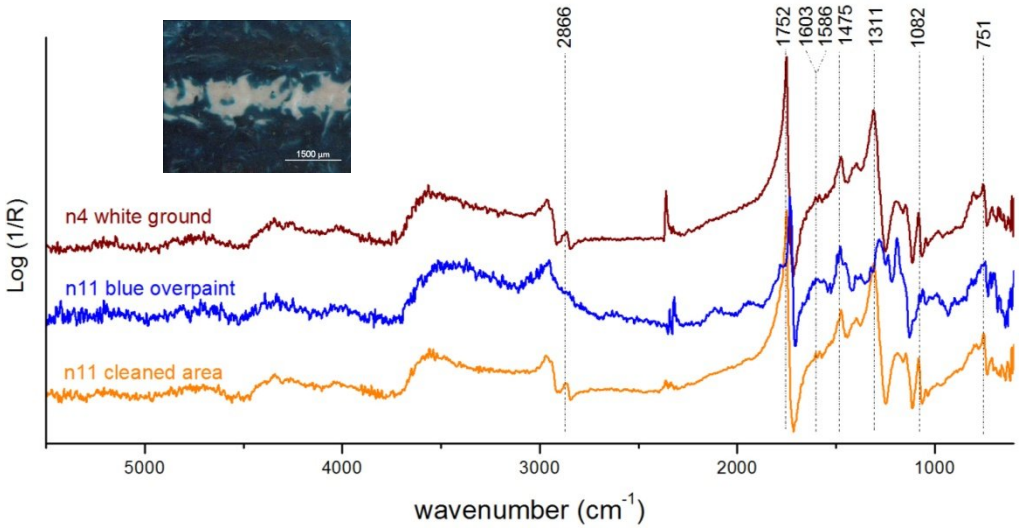

Figure 17 – Reflection micro-FTIR spectrum of a cleaned area in n11 paint using the excimer KrF laser at λ = 248 nm (t_p = 30 ns, 3.06 J·cm^{-2}, 30 pulses) compared with standard spectra of n11 overpaint and white ground.

About the use of the Nd:YAG laser at λ = 355 nm and t_p = 150 ps on this mock-up, the analyses show that the results were not so satisfactory as it were for the mock-up#1, since in most cases cleaning was incomplete and in cases where laser could remove the overpaint, the white ground was no longer visible, showing canvas exposure. This can possibly be explained by the fact that the white ground layer is too much thin, and, adding to this, the laser at 355 nm is absorbed less by the material to be removed and, due to that, had a deeper penetration on the substrate.

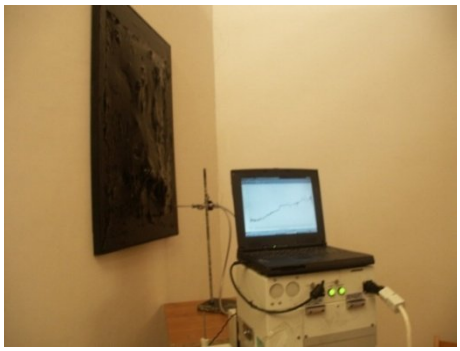

Figure 18 – Fibre-optics FTIR spectroscopy portable equipment. Photo courtesy of SMAArt (Perugia).

The fibre-optics portable equipment (figure 18) has given acceptable results, in sense that the spectra obtained could be compared with the ones from bench equipment. The only disadvantages found are related to the analysed spot diameter, which is around 4 mm. I can be too big to analyse ablated areas from Nd:YAG 355 nm and excimer KrF laser 248 nm. Other disadvantage is spectra range, which is in theory 7000-900 cm^{-1}. However, in practice the background spectra obtained is not perfect. In fact, the fibres show a Se-H stretching absorption in the 2050-2250 cm^{-1} range altering the signal to noise ratio in that region. Environmental moisture at 3100–3500 cm^{-1} and carbon dioxide at 2250 cm^{-1} can also cause interference, blinding the regions. Also, below ≈1000 cm^{-1} the spectra are indiscernible. This feature can be a problem considering for example the characteristic silicate band of ultramarine blue, which in the reflection spectra has a *reststrahlen* inversion band at about 1000 cm^{-1}, or, for example, the aromatic C-H out-of-plan bands characteristic of styrene acrylics at 746 cm^{-1} and 698 cm^{-1}.

In figure 19, reflection FTIR spectra from the portable equipment are presented, giving examples of aggressive cleaning and incomplete cleaning compared with overpaint, white ground and canvas standard spectra. In the example of incomplete cleaning an OM image of the cleaned area is shown to explain the difficulty in assessing visually the efficiency of overpaint removal. In fact, the image suggests that the overpaint was removed.

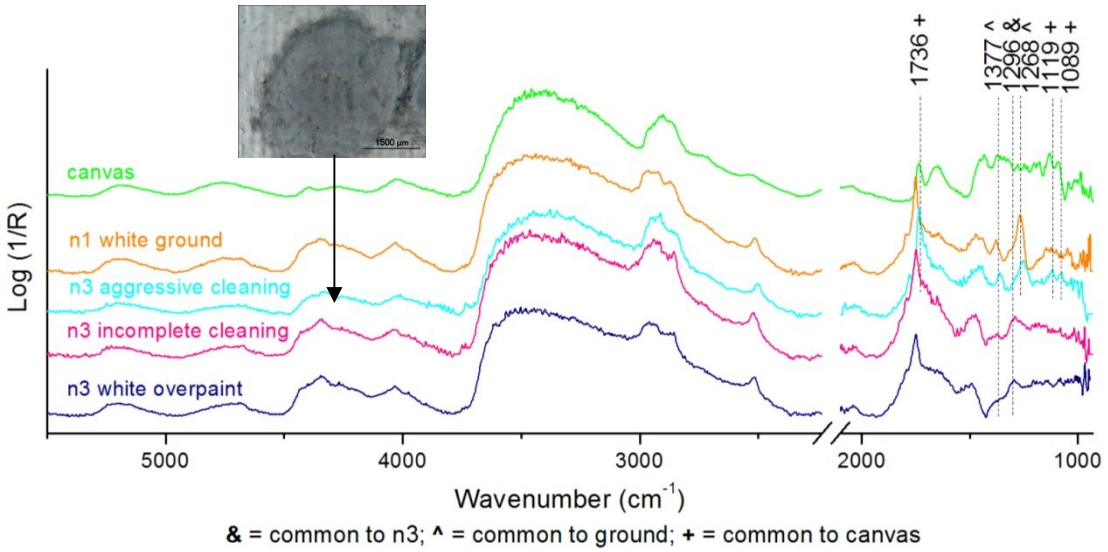

Figure 19 – Reflection FTIR spectra, showing examples of aggressive and incomplete cleaning, by comparison with n3 overpaint, white ground and canvas standard spectra.

- Raman spectroscopy. This spectroscopic technique permitted to observe some of the alterations phases formed and some molecular alterations on paint materials after laser irradiation. In most cases, analysis made in the micro black particles observed with OM showed the presence of carbon (figure 20), meaning that probably it is an alteration phase from the binder degradation.

However, not all ablation areas showed the presence of carbon on Raman spectroscopy, even if the greyish discoloration is visible. This may be explained by the sensitivity of the spectroscopic equipment, meaning that the black particles are too little to be analysed alone without the interference of the dominant white zone.

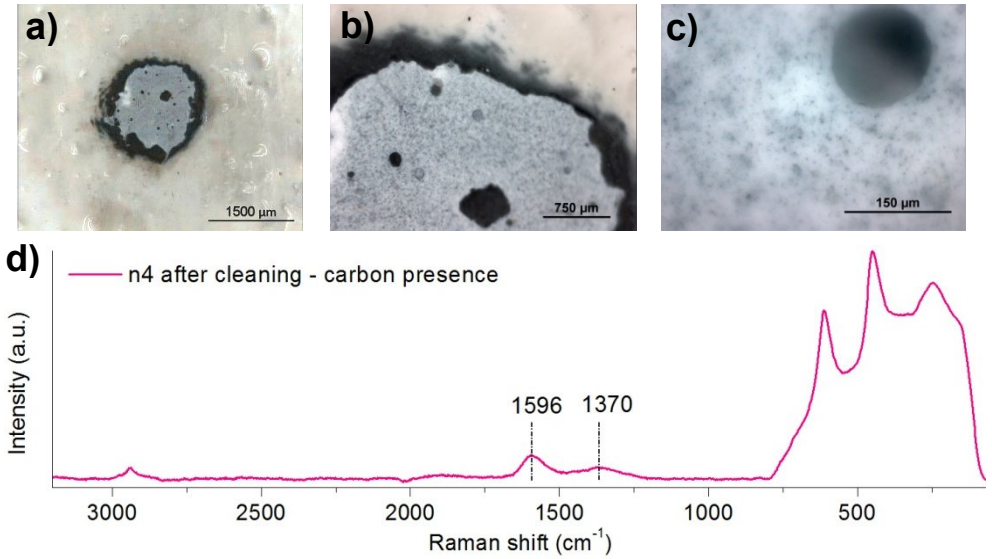

Figure 20 – Ablation in paint n4 using the Nd:YAG 355 nm laser, t_p = 10 ns, F = 2.06 J·cm^{-2} and 10 pulses, a) the fibre-optics portable video microscopy image from cleaned area, b) and c) optical microscopy images showing the micro black particles, d) micro-Raman spectrum (λ=532 nm) of this area with carbon assignment bands.

Considering that this effect only is visible in the white paints (the corresponding blue paints with the same binders did not shown signs of binder degradation upon irradiation), titanium dioxide may play a main role on this effect. In the literature, TiO_2 is characterised by the presence of photoinduced phenomena, which are originate from the semiconductor band gap, and can lead to photocatalysis.

Thus, this phenomenon may be responsible for the photodegeneration of organic compounds [40] (for more information on the photocatalyst properties of TiO_2 see appendix 2, page A9).

Adding to this, a small but significant alteration of the relative intensity of the Raman bands of rutile has been observed upon laser interaction. The obtained spectra permitted to see a relative decreasing of the band assigned to vibrational group A_{1g} in respect to the other signs of the rutile (see figure 21). Several analyses were made on the ablated areas to evaluate this decrease, and a systematic result was found, i.e. every laser system produced this effect on titanium white (rutile) pigment, when the white paint was found greyish. Further, the lasers with wavelengths 1064 nm and 355 nm showed in almost every case the more and less decrease of this vibrational band, respectively.

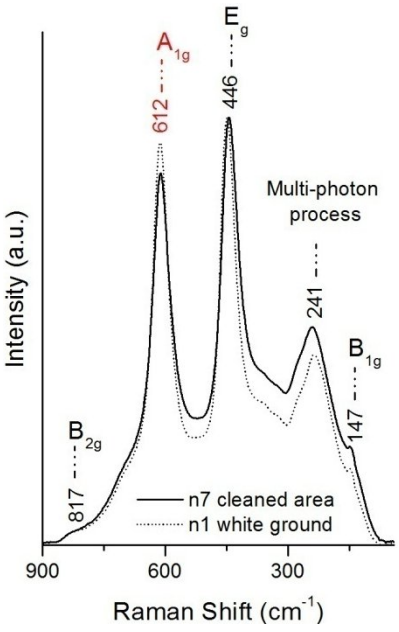

Figure 21 – Raman spectra (λ=532 nm) of a cleaned area on n7 paint and the standard for white ground (rutile) for comparison (normalized [0,1]) [41].

In this paper [41] the same effect was found on the same vibrational group upon laser irradiation. Since the mock-ups in this paper were TiO_2 single crystals (40 mm in diameter and 1.5 mm thick) and the energy densities applied were much higher, at the end of the experiment the complete alteration from rutile structure to anatase was observed. However, in the results observed in the current work, because of the low titanium dioxide concentration (it is dispersed in the binder), in respect to the mock-up in that experience, the alteration process from rutile to anatase structure may not be complete.

In what concerns the blue pigments they did not show any significant alteration in Raman spectra that could be associated to a crystalline or molecular change. The observed changes in the spectra were only related to the absolute intensity. However, it must be reported that in the case of phthalocyanine blues an increase in the fluorescence background has been observed on the borders of the cleaned areas, probably suggesting the production of degradation products (see example in figure 22). This fluorescence is not equal in all phthalocyanine blues. In the n10 paint an accentuated fluorescence is observed very close to the laser irradiation line (532 nm) that possibly is deformed by the Raman notch. In the n11 paint there are two main relevant fluorescence bands that in wavelength correspond to absorptions around 667 nm and 617 nm. On the other hand, the analysis made on n12 paint, the dioxazine violet, did not show any significant alteration in the fluorescence.

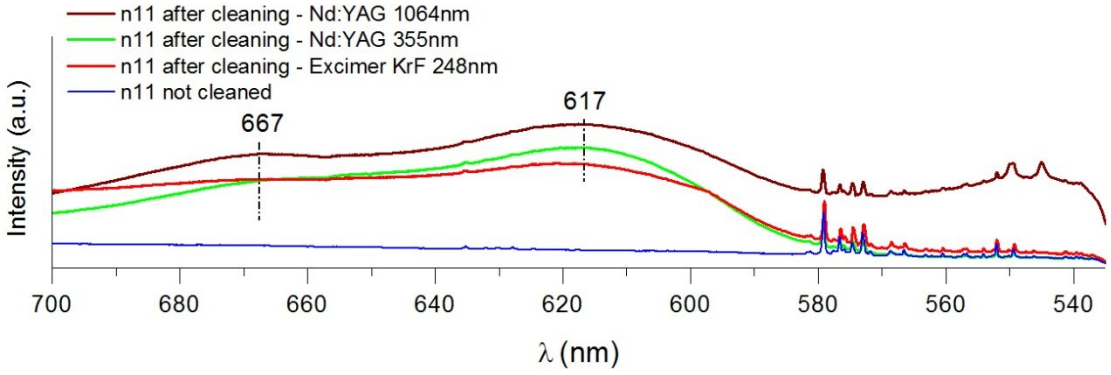

Figure 22 – Micro-Raman spectra (λ=532 nm) of phthalocyanine paint n11, performed in the remaining blue spots on the ablation areas, which showed notable fluorescence around 667 nm and 617 nm.

In what concerns the ultramarine blues the relative intensity between the bands assigned to the chromophores S^{2-} and S^{3-}, namely the scattering at 581 cm^{-1} and 549 cm^{-1}, respectively, did not alter whatsoever. It was expected that chromophores would degrade first than the aluminosilicate matrix due to their removal from the sodalite cage. However, by analyses made with micro-Raman, when the chromophores were not visible anymore, also the assignment band of silicate in micro-FTIR was not visible. In fact, it has been demonstrated that this pigment is very stable to laser irradiation, suffering discoloration only at very high energy densities [23].

In respect of the fibre-optics Raman spectroscopy portable equipment (figure 23), it was not possible to identify the presence of carbon. In fact, the micro black particles are too little to be analysed without interference from the white paint matrix. However, the rutile alteration could be seen as well as the absolute decrease of the assignment bands of the phthalocyanine (figure 24) and dioxazine. In this case the use of the laser λ=785 nm in the analysis showed the best results.

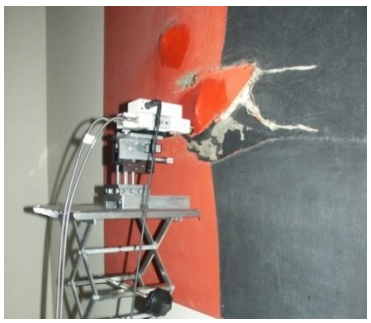

Figure 23 – Fibre-optics Raman spectroscopy portable equipment. Photo courtesy of SMAArt (Perugia)

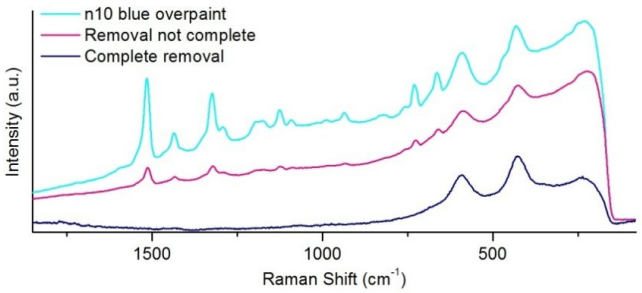

Figure 24 – Raman spectra (λ=785 nm) of two different ablation areas on paint n10 containing phthalocyanine blue, one successful, and other incomplete, compared with the standard spectrum of the overpaint.

In the following table, the general results on the effectiveness and harmfulness of laser cleaning are presented, taking into account the analyses made with OM, FTIR and Raman spectroscopies. In each case a singular ablation area (with specific laser parameters) was chosen, considering it as the one where the cleaning was more efficient with that specific laser system. The same table, yet more detailed, is presented in the appendix 3 (page A10), with information added on laser parameters (fluence and number of pulses), fibre-optics video microscopy image, and observations.

Table 4 – General results for laser cleaning experiment on mock-up #1 and #4 using different laser systems. The n1 and the n4 are the original layers except in its specific row where the canvas is considered the original layer.

Canvas mock-up	#1					#4	
Laser system / **Paint**	Nd:YAG λ=1064 nm t_p=10 ns	Nd:YAG λ=532 nm t_p=10 ns	Nd:YAG λ=355 nm t_p=10 ns	Nd:YAG λ=355 nm t_p=150 ps	Excimer KrF λ=248 nm t_p=30 ns	Nd:YAG λ=355 nm t_p=150 ps	Excimer KrF λ=248 nm t_p=30 ns
n1 - Polycolor®	- *	- *	- *	- *	- *	++ *!	+ *
n2 - Liquitex®	- *	+ !!	+++ !	++ *!	- *	++ *!	++ *
n3 - Griffin®	+++ !!	+ !!	+++ *!	++ !	- *	++ *!	++ *
n4 - Boero®	- !!	++ *!!	+++ *!	+++ !	+ *!	+++ *!	n.t.
n5 - Fly color®	-	- *	++ !	+++ !	- *	++ *!	++ *
n6 - Belton®	++ !	+ *!	+++ *!	++ !	-	+ *!!	+ *
n7 - Polycolor®	+++ !!	++ !	+++	+++ !	++ !	++ !!	++
n8 - Liquitex®	+++ !!	+++ !	+++ !	+++ !	++ !	++ !!	+++
n9 - Griffin®	+++ !!	n.t.	+++ !	++ !	++ !	++ !!	++
n10 - Boero®	+++ !!	n.t.	+++ !	++	++	++ !!	++
n11 - Fly color®	+++ !!	n.t.	+++	++	+++	++ !!	+++
n12 - Belton®	+++ !!	n.t.	+++	++	+++	++ !!	++ *

(-) no removal; (+) minor removal; (++) significant removal but with several overpaint residuals; (+++) total removal; (*) damage/alteration to the overpaint; (!) damage/alteration to the ground layer; (!!) aggressive ablation; (n.t.) not tested.

As it is possible to observe in the table, the lasers Nd:YAG 355 nm (t_p = 10 ns and t_p = 150 ps) at rather high energy densities and several pulses (≈10 for the ns regime and ≈20 for the ps regime) showed the best results for the mock-up #1. On the contrary, the excimer KrF laser 248 nm (t_p = 30 ns) showed to be the best choice in the mock-up #4, using energy densities around 3 $J \cdot cm^{-2}$ and ≈30 pulses.

One possibility for the control of the most complicated side-effect found in this laser experiment, the greyish discoloration, can be the use of ultra-short laser systems, which were not tested in this work. Generally, the ns (nanosecond) cleaning regime gives photo-thermal phenomena, which are reduced upon ultra-short irradiation (i.e. picosencond - ps, femtosencond - fs), as confirmed from many studies [11,34,42-44]. In fact, these ultra-short lasers allow minimal thermal diffusion, heat accumulation after each pulse given, and the ablation morphology can be superior to that obtained with nanosecond laser pulses, mainly with the femtosecond lasers.

However, there are other conditions that influence the photo-thermal, photo-chemical or photo-mechanical damages of original layers, and govern on which of them will be more dominant. Firstly, it is important to choose the most appropriate wavelength, and whether is weakly or strongly absorbed by the paint material. In theory, the wavelengths more adapted for painted artworks are the ones ≤ 248 nm, to achieve a layer-by-layer removal. On the other hand, UV lasers are more capable to break the bonds of the polymer chains and will induce photo-chemical activity, while lasers with wavelengths of 1064 nm and 532 nm will mainly remove the material by explosive vaporization. It must also be appointed the importance of the original layer absorption in the electromagnetic spectrum, since this will influence substantially the cleaning process, mainly if the overpaint is very thin or does not absorb strongly.

3. Conclusions

The optical and spectroscopic analyses permitted the evaluation of the effectiveness and harmfulness of the different cleaning methods tested.

On the chemical cleaning control the analytical approach lead to the conclusion that acetone was the most efficient solvent, yet with strong action and deep penetration into substrate. Next in the line of efficacy is ethyl lactate, which seemed to allow more control in the cleaning, yet still leaving several overpaint residues behind. The considered medium-efficient solvents were ethanol, isopropyl alcohol, and xylene by giving partial cleaning or minor removal of the overpaints. The solvents and chemical systems that were not able to remove the overpaints were deionized water, ammonium and petroleum ether. To sum up, chemical cleaning has demonstrated to give several problems for the selective removal of overpaints.

Regarding the effectiveness of the laser cleaning method it is possible to highlight the following points. The Nd:YAG laser 1064 nm has proven to be a very aggressive irradiation regime within the parameters used. The hazard effects observed were the discoloration of the white paints, changes in the substrate morphology and the uncontrolled removal of overpaints, with canvas exposure in the majority of cases. The same laser at λ = 532 nm has shown to be the less efficient and, therefore, further research should be carried out by decreasing the energy density and increasing the number of pulses. On the contrary, laser regimes of λ = 355 nm and λ = 248 nm demonstrated to be the most

efficient and harmless, which in the case of mock-up n1 the most efficient was the Nd:YAG 355 nm, while in mock-up n4 the most efficient was the excimer KrF 248 nm.

The alterations observed on paint materials under laser irradiation were mainly the greyish discoloration of the white paints in every cleaning parameter, possible caused by the photocatalyst action of titanium white on the organic binder, leading to its degradation and the formation of carbon. On the other hand, titanium white itself showed alteration in its Raman spectrum, leading to believe that during laser irradiation, the structure of rutile tended to change to the anatase form, even if this change was not observed until its final stage. Hence, when considering laser cleaning one must play full attention as to whether titanium white is present, since there are still no alternative solutions for this structural modification and for the darkish discoloration effect.

Another important issue to consider is that several active side radicals may remain on the original painted surface when polymeric bonds are broke under laser irradiation, and, therefore, can do harm to original paint in long term. Further research should be developed on this matter.

Furthermore, it must be considered that this work is part of a preliminary stage, where one of the main aims was to evaluate the limitations of the laser cleaning method on modern and contemporary paintings, in order to calculate damage thresholds and decide on cleaning parameters. Therefore, further research will focus on experimenting well defined cleaning parameters, with the aim of improving a laser system in order to resolve all issues appointed in this work.

In conclusion, the spectroscopic protocol has proven to be successful, by the satisfactory results with the mock-ups analyses, offering the possibility to select the best cleaning parameters. In fact, micro-FTIR and the optical microscopy were very useful techniques to evaluate the combined cleaning effectiveness and harmfulness. On the other hand, Raman spectroscopy offered the possibility to evaluate the possible chemical or structural alteration effects on pigments upon laser cleaning. Furthermore concerning the fibre-optics FTIR portable equipment, the results achieved are considered comparable to the ones from bench equipment. As for fibre-optics Raman portable equipment, the results were not satisfactory, due to the interference with the material that surrounds the analysed area, since the experimental set-up does not permit a confocal analysis.

4. References

[1] Pacht, O., *Van Eyck and the Founders of Early Netherlandish Painting*, Harvey Miller Publishers, Munich (1999).

[2] Learner, T., 'Modern Paints', in *Sackler NAS Colloquium, Scientific Examination of Art: Modern Techniques in Conservation and Analysis*, National Academy of Sciences (2005) 137-151. ISBN: 0-309-54961-2. Retrieved June 10, 2010 from: http://www.nap.edu/catalog/11413.html.

[3] Learner, T. J. S., *Analysis of Modern Paints*, Getty Conservation Institute, Los Angeles (2004), 81-116.

[4] Kahrim, K., *New methodologies for in situ non invasive spectroscopic analyses of 20th century synthetic painting materials*, PhD dissertation, Università Degli Studi di Perugia, Perugia (2009), pp 10-97.

[5] Lefranc & Bourgeois, *Peinture vinylique extra-fine Flashe*, retrieved June 10, 2010, from: http://www.lefranc-bourgeois.com/beaux-arts/produits-acryliques-vinyliqueflashe.html.

[6] Encyclopædia Britannica, *Nitrocellulose*, retrieved June 10, 2010, from: http://www.britannica.com/EBchecked/topic/416152/nitrocellulose.

[7] Jablonski, E., Learner, T., Hayes, J., Golden, M., 'Conservation concerns for acrylic emulsion paints: a literature review', in Tate's online research journal (Autumn 2004). ISSN 1753-9854. Retrieved in October 7, 2009 from: http://www.tate.org.uk/research/tateresearch/tatepapers/04autumn/jablonski.htm.

[8] Scholten, J.H., Teule, J.M., Zafiropulos, V., Heeren, R.M.A., 'Controlled laser cleaning of painted artworks using accurate beam manipulation and on-line LIBS-detection', *J. Cult. Heritage* **1** (2000) S215-S220.

[9] Bordalo, R., Morais, P. J., Gouveia, H., Young, C., 'Laser cleaning of easel paintings: an overview', *Laser Chemistry* Article ID **90279** (2006) 9 pages.

[10] Marczak, J., Koss, A., Targowski, P., Góra, M., Strzelec, M., Sarzyński, A., Skrzeczanowski, W., Ostrowski, R., Rycyk, A., 'Characterization of Laser Cleaning of Artworks', *Sensors* **8** (2008) 6507-6548.

[11] Rode, A. V., Baldwin, K. G. H., Wain, A., Madsen, N. R., Freeman, D., Delaporte, Ph., Luther-Davies, B., 'Ultrafast laser ablation for restoration of heritage objects', *Applied Surface Science* **254** (2008) 3137–3146.

[12] Melessanaki, K., Stringari, C., Fotakis, C., Anglos, D., 'Laser cleaning and spectroscopy: a synergistic approach in the conservation of a modern painting', *Laser Chemistry* Article ID **42709** (2006) 5 pages.

[13] Pouli, P., Selimis, A., Georgiou, S., Fotakis, C., 'Recent studies of laser science in paintings conservation and research', *Accounts of Chemical Research* **43(6)** (2010) 771-781.

[14] Real, W. A., Zergioti, I., Spetsidou, Y., Anglos, D., 'Use of KrF excimer laser for cleaning fragile and problematic paint surfaces', in *11th triennial meeting of the International Council of Museums Comittee for Conservation*, *Edinburgh, Scotland, 1-6 September 1996*, ed. Bridgland, J., James X James, London (1996) Vol. I 303-309.

[15] Greenemeier, L., 'Deconstructing art to save it: laser analysis tested to restore paintings', *Scientific American*, (July 9, 2008). Retrieved June 7, 2010 from: http://www.scientificamerican.com/article.cfm?id=deconstructing-art-to-save.

[16] Salimbeni, R., Pini, R., Siano, S., 'Achievement of optimum laser cleaning in the restoration of artworks: expected improvements by on-line optical diagnostics', *Spectrochimica Acta Part B* **56** (2001) 877-885.

[17] Andreoni, A., Sliwinski, G., 'Laser – Fundamentals', in *Handbook on the use of Lasers in Conservation and Conservation Science*, COST office, Brussels (2008), e-version ISBN-10: 973 88109 30. Retrieved March 8, 2010 from http://alpha1.infim.ro/cost/pagini/handbook/index.htm.

[18] Abraham, M., Twilley, J., 'A review of the state of the art of laser cleaning in conservation', The Los Angeles County Museum of Art, Los Angeles (1997) 12-14.

[19] Oujja, M., Rebollar, E., Castillejo, M., 'Spectroscopic studies of laser ablation plumes of artwork materials', *Applied Surface Science* **211** (2003) 128–135.

[20] Pouli, P., 'Lasers in art conservation. State of the art on the fundamental research and the applications carried out at FORTH-IESL', *Foundation for Research and Technology-Hellas*, retrieved in January 15, 2010 from: http://www.arcchip.cz/w12/w12_pouli.pdf.

[21] Schnell, A., Goretzki, L., Kaps, C., 'Nd-YAG laser irradiation of pigments and binders in paint layers', in *EUROMAT 2003, Symposium P2 - Materials and Conservation of Cultural Heritage, EPFL-Lausanne*, Scholarly Essay, GRIN (2003) 1-5. ISBN 978-3-638-06310-4.

[22] Castillejo, M., Martín, M., Oujja, M., Rebollar, E., Domingo, C., García-Ramos, J. V., Sánchez-Cortés, S., 'Effect of wavelength on the laser cleaning of polychromes on wood', *Journal of Cultural Heritage* **4** (2003) 243–249.

[23] Chappé, M., Hildenhagen, J., Dickmann, K., Bredol, M., 'Laser irradiation of medieval pigments at IR, VIS and UV wavelengths', *Journal of Cultural Heritage* **4** (2003) 264s–270s.

[24] Georgiou, S., Zafiropulos, V., Anglos, D., Balas, C., Tornari, V., Fotakis, C., 'Excimer laser restoration of painted artworks: procedures, mechanisms and effects', *Applied Surface Science* **127–129** (1998) 738–745.

[25] Castillejo, M., Martín, M., Oujja, M., Silva, D., Torres, R., Manousaki, A., Zafiropulos, V., van den Brink, O. F., Heeren, R. M. A., Teule, R., Silva, A., Gouveia, H., 'Analytical study of the chemical and physical changes induced by KrF laser cleaning of tempera paints', *Anal. Chem*. **74** (2002) 4662-4671.

[26] de Cruz, A., Wolbarsht, M. L., Hauger, S. A., 'Laser removal of contaminants from painted surfaces', *Journal of Cultural Heritage* **1** (2000) S173–S180.

[27] Bracco, P., Lanterna, G., Matteini, M., Nakahara, K., Sartiani, O., de Cruz, A., Wolbarsht, M. L., Adamkiewicz, E., Colombini, M. P., 'Er:YAG laser: an innovative tool for controlled cleaning of old paintings: testing and evaluation', *Journal of Cultural Heritage* **4** (2003) 202s–208s.

[28] Meilunas, R. J., 'The application of diffuse reflectance infra-red Fourier transform spectroscopy to the analysis of paint surfaces', bachelor thesis, Massachusetts Institute of Technology, Massachusetts (1986), pp 16-36.

[29] Zeine, C., Grobe, J., 'Diffuse reflectance infrared Fourier transform (DRIFT) spectroscopy in the preservation of historical monuments: studies on salt migration', *Mikrochim. Acta* **125** (1997) 279-282.

[30] Wijnja, H., Schulthess, C. P., 'ATR-FTIR and DRIFT spectroscopy of carbonate species at the aged γ-Al_2O_3/water interface', *Spectrochimica Acta Part A* **55** (1999) 861-872.

[31] Ciliberto, E., Spoto, G., 'Modern analytical methods in art and archaeology', Jonh Wiley & Sons, Inc., New York (2000), 255-274, ISBN 0-471-29361-X.

[32] Röseler, A., Korte, E.-H., 'Reflection anomalies related to n = 1', *Vibrational Spectroscopy* **43** (2007) 111–115.

[33] Miliani, C., Rosi, F., Brunetti, B. G., Sgamellotti, A., 'In situ noninvasive study of artworks: the MOLAB multitechnique approach', *Accounts of Chemical Research* **Vol. 43(6)** (2010) 728-738.

[34] Rosi, F., Daveri, A., Doherty, B., Nazzareni, S., Brunetti, B.G., Sgamellotti, A., Miliani, C., 'On the use of overtone and combination bands for the analysis of the $CaSO_4$–H_2O system by mid-infrared reflection spectroscopy', *Applied Spectroscopy* **Vol. 64(8)** (2010) 956-963.

[35] Pouli, P., Paun, I.-A., Bounos, G., Georgiou, S., Fotakis, C., 'The potential of UV femtosecond laser ablation for varnish removal in the restoration of painted works of art' *Applied Surface Science* **254** (2008) 6875–6879.

[36] Castillejo, M., Martín, M., Oujja, M., Santamaría, J., Silva, D., Torres, R., Manousaki, A., Zafiropulos, V., van den Brink, O. F., Heeren, R. M. A., Teule, R., Silva, A., 'Evaluation of the chemical and physical changes induced by KrF laser irradiation of tempera paints', *Journal of Cultural Heritage* **4** (2003) 257s–263s

[37] Ormsby, B., Kampasakali, E., Miliani, C., Learner, T., 'An FTIR-based exploration of the effects of wet cleaning treatments on artists' acrylic emulsion paint films', *e-Preservation science* **6** (2009) 186-195.

[38] Kahrim, K., Daveri, A., Rocchi, P., de Cesare, G., Cartechini, L., Miliani, C., Brunetti, B. G., Sgamellotti, A., The application of in situ mid-FTIR fibre-optic reflectance spectroscopy and GC–MS analysis to monitor and evaluate painting cleaning', *Spectrochimica Acta Part A* **74** (2009) 1182–1188.

[39] Scheerer, S., Abraham, M., Madden, O., 'Study of the effects of laser radiation on epoxy resins and epoxy systems on stone, ceramic, and glass surfaces', *Journal of Cultural Heritage* **4** (2003) 223s–229s.

[40] Carp, O., Huisman, C. L., Reller, A., 'Photoinduced reactivity of titanium dioxide', *Progress in Solid State Chemistry* **32** (2004) 33-177.

[41] Ma, H. L., Yang, J. Y., Dai, Y., Zhang, Y. B., Lu, B., Ma, G. H., 'Raman study of phase transformation of TiO_2 rutile single crystal irradiated by infrared femtosecond laser', *Applied Surface Science* **253** (2007) 7497–7500.

[42] Dumitru, G., Romano, V., Weber, H. P., Sentis, M., Marine, W., 'Femtosecond ablation of ultrahard materials', *Appl. Phys. A* **74** (2002) 729-239.

[43] Rode, A. V., Freeman, D., Baldwin, K. G. H., Wain, A., 'Scanning the laser beam for ultrafast pulse laser cleaning of paint', *Appl. Phys. A* **93** (2008) 135-139.

[44] Gaspard, S., Oujja, M., Moreno, P., Méndez, C., García, A., Domingo, C., Castillejo, M., 'Interaction of femtosecond laser pulses with tempera paints', *Applied Surface Science*, **255** (2008) 2675-2681.

APPENDICES

Appendix 1 - Materials and methods

- Canvases mock-ups. Six painted cotton canvases on stretcher with ≈29x25 cm^2 were prepared in May 2009 at the Istituto Superiore per la Conservazione ed il Restauro in Roma (ISCR). The paint layers were produced with commercial paint formulations using two colours and six different binders giving a total of 12 products (six white, six blue, repeating the binders on each combination blue/white). The white ground was prepared using the white paints over which was applied a second paint layer, squared shape (≈4.5x4.5 cm^2), with the remaining 11 other selected products (the other five whites and six blue). From all six canvases, only five were used in this work, that is, the first four were cleaned with different lasers, and the mock-up #6 was cleaned with different solvents (the mock-up #5 was not cleaned and therefore was not sent from the ISCR to be analysed). In figure a1 and figure a2 all the mock-ups analysed can be seen.

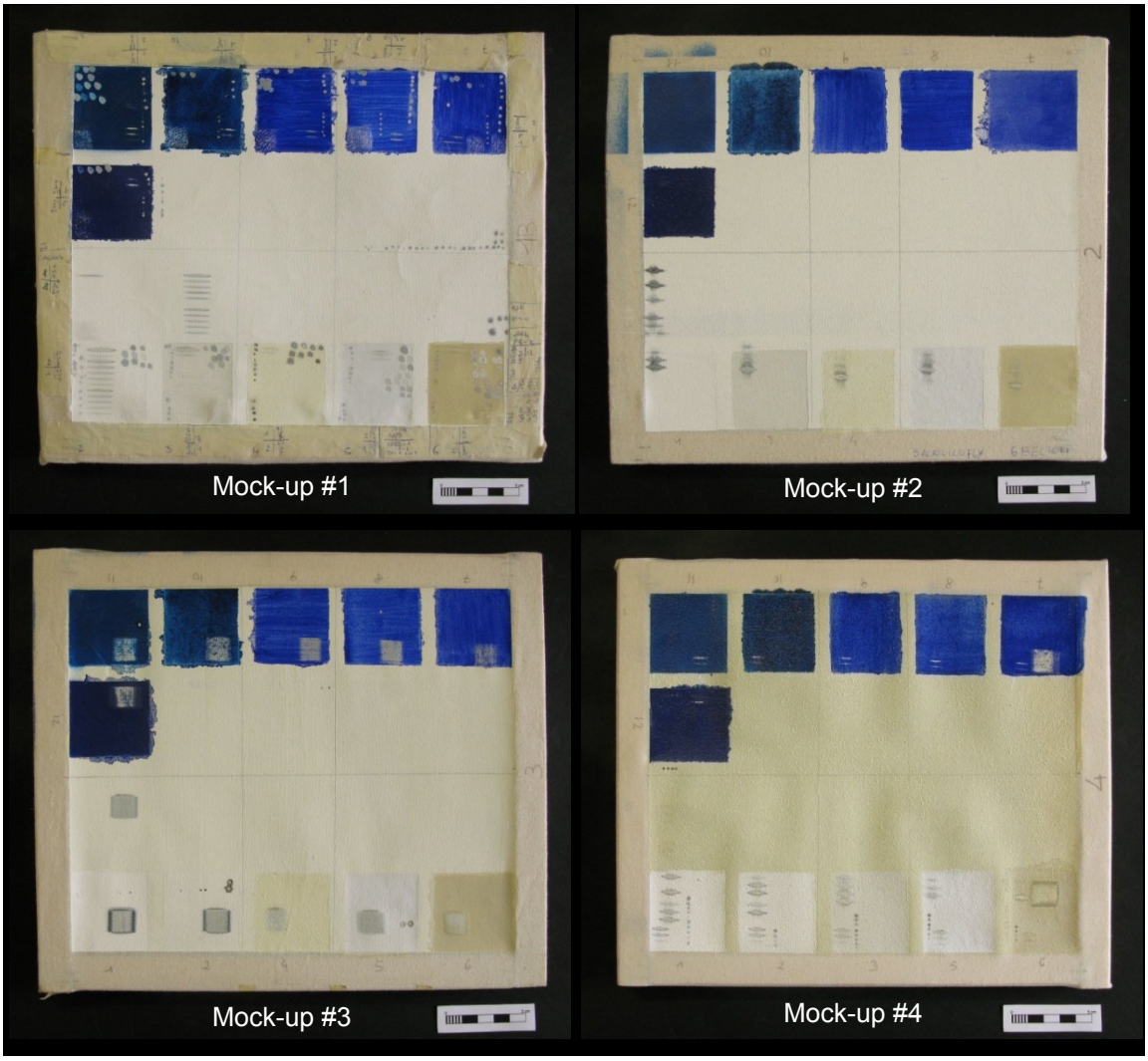

Figure a1 – Mock-ups #1 to #4 used for the study on the laser cleaning method effectiveness.

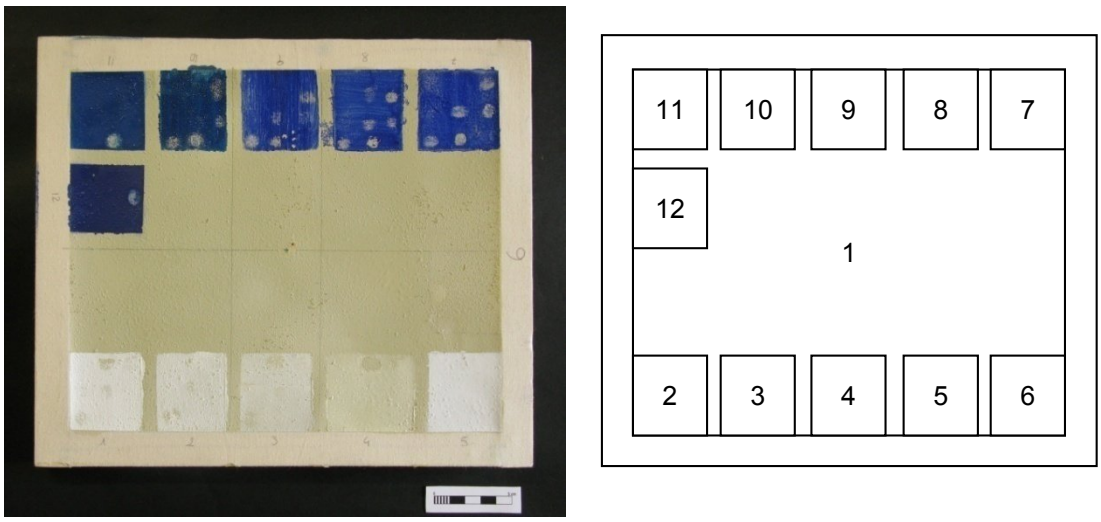

Figure a2 – Mock-up #6 used for the study on the solvent cleaning effectiveness (left). Numeration of the different kinds of commercial paint formulations as they are organised in the mock-up#1 (right).

- Characterisation of commercial paints (pigments, extenders and paint mediums). Information on the chemical composition of commercial paints used for the mock-up preparation is reported in table a1, resulting from both technical sheet and spectroscopic analysis. The numeration of the paints is correlated to the right image in figure a2.

Table a1 - The 12 commercial paint formulations used in the mock-ups.

Commercial paint	White colours		Blue colours		Paint medium
	Pigments	Extenders	Pigments	Extenders	
Polycolor®, Maimeri *artist's use*	**1 –** Titanium white (rutile)	$CaCO_3$	**7 –** Ultramarine blue (with kaolin)	$CaCO_3$	PVA/VeoVa
Liquitex®, Permanent Pigments Inc *artist's use*	**2 –** Titanium white (rutile)	$CaCO_3$	**8 –** Ultramarine blue (with kaolin)	$CaCO_3$	PEA-MMA
Griffin®, Winsor & Newton *artist's use*	**3 –** Titanium white (rutile)	$CaCO_3$	**9 –** Ultramarine blue (with kaolin)	$CaCO_3$	Alkyd
Boero®, Boero Bartolomeo *household*	**4 –** Titanium white (rutile)	-	**10 –** Phthalocyanine blue*	-	Alkyd
Fly Color®, Motip Dupli Group *household*	**5 –** Titanium white (rutile)	-	**11 –** Phthalocyanine and dioxazine**	-	Styrene-acrylic copolymer
Belton Molotow®, Art primo *household*	**6 –** Titanium white (rutile), and iron component	-	**12 –** Dioxazine violet***	-	Nitrocellulose and alkyd

* Phthalocyanine PB15:6 C.I. 74160:6 [1]
** Pigment mixture: PB15:6 and PV23
*** Dioxazine violet PV23 C.I. 51319 [1]

[1] Scherrer, N. C., Stefan, Z., Francoise, D., Annette, F., Renate, K., 'Synthetic organic pigments of the 20th and 21st century relevant to artist's paints: Raman spectra reference collection', *Spectrochimica Acta Part A* **73** (2009) 505–524.

Titanium dioxide (rutile) is present in all the white paints as the main pigment. However, the paint n6 has also an iron component, identified with the X-ray fluorescence analysis. In what concerns the blue layers there are more variety of pigments, i.e. three different pigments were well-identified, namely ultramarine blue, phthalocyanine blue and dioxazine violet. This last one, however, is not a blue pigment and no other pigment in the mixture was identified. Nevertheless, the paint has a blue tone. One of the blue paints has a mixture of the phthalocyanine and the dioxazine pigments. The Raman spectra of all pigments identified are showed in figure a3.

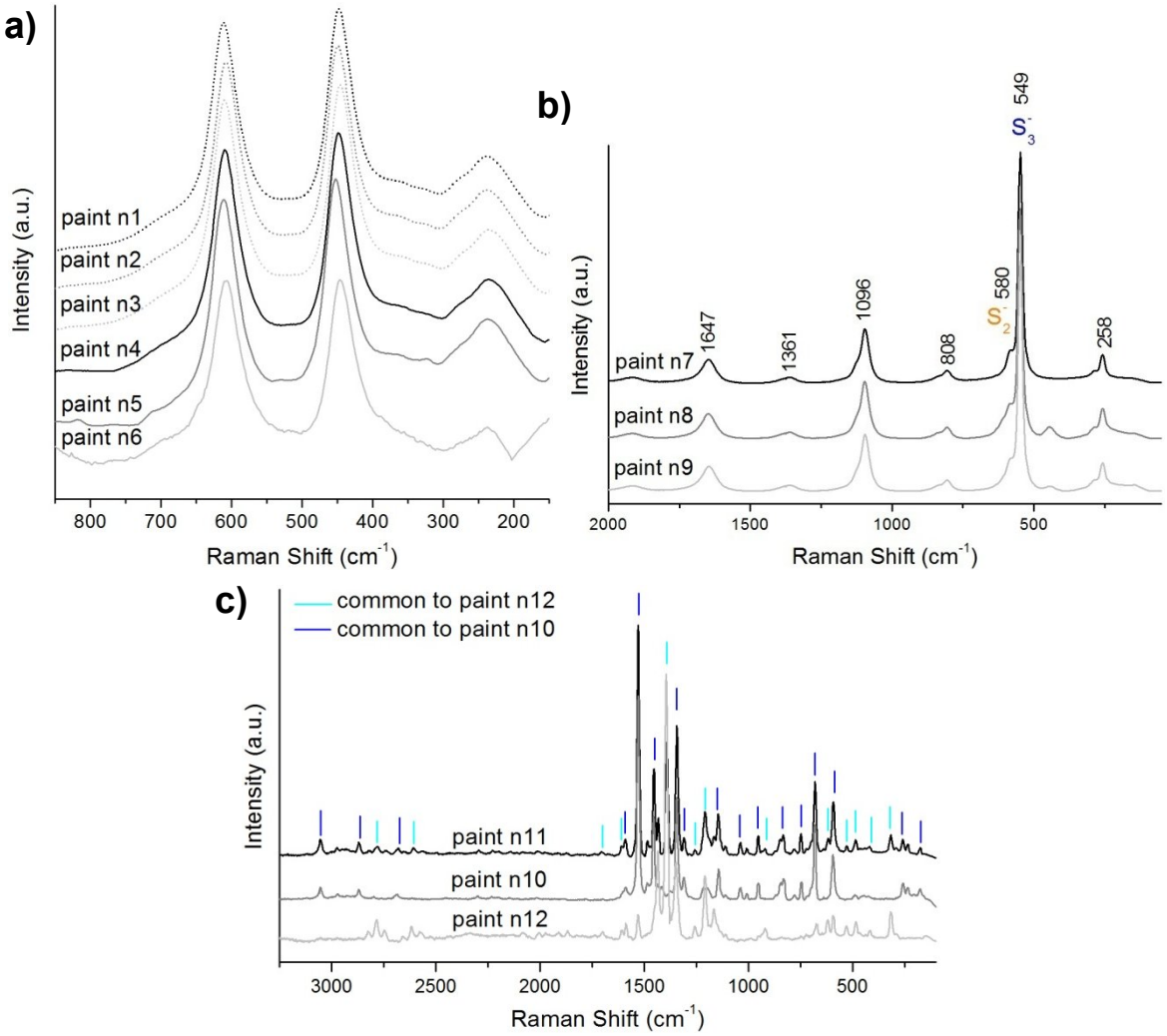

Figure a3 – Raman spectra of all commercial paint formulations involved in this study. a) All white paints showed titanium white (rutile) as the dominant pigment. b) Three blue paints showed the presence of ultramarine blue. c) The other three blue paints showed different spectra: one corresponding to a phthalocyanine blue (paint n10); other to a dioxazine violet (paint n12); and other to a mixture between these two organic pigments (paint n11).

In what concerns binders identification, the information given by the technical sheet was confirmed by FTIR analysis in transmission mode (KBr pellets), and then compared with the spectra obtained in reflection mode using bench and portable equipment to sustain the results presented in this work. In figure a4 all the different six binders presented in the paints are shown, by analyses on the six different white paints, with the evidenced assignment bands that permit their identification.

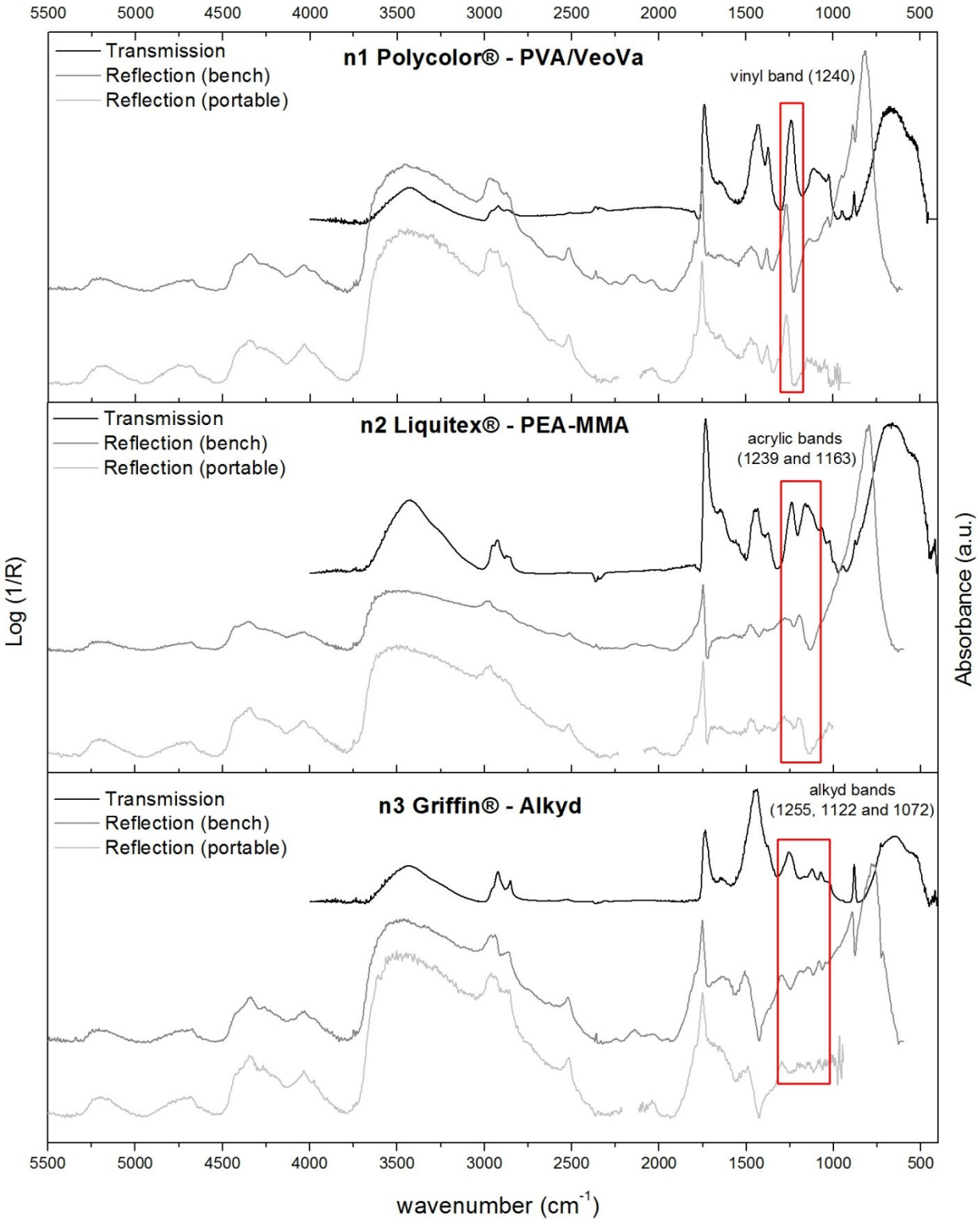

Figure a4 – FTIR spectra of all commercial white paint formulations studied where binders were indentified. The spectra are presented in transmission and in reflection mode (with bench and portable equipment), for each white paint. The most important bands are assigned for each binder.

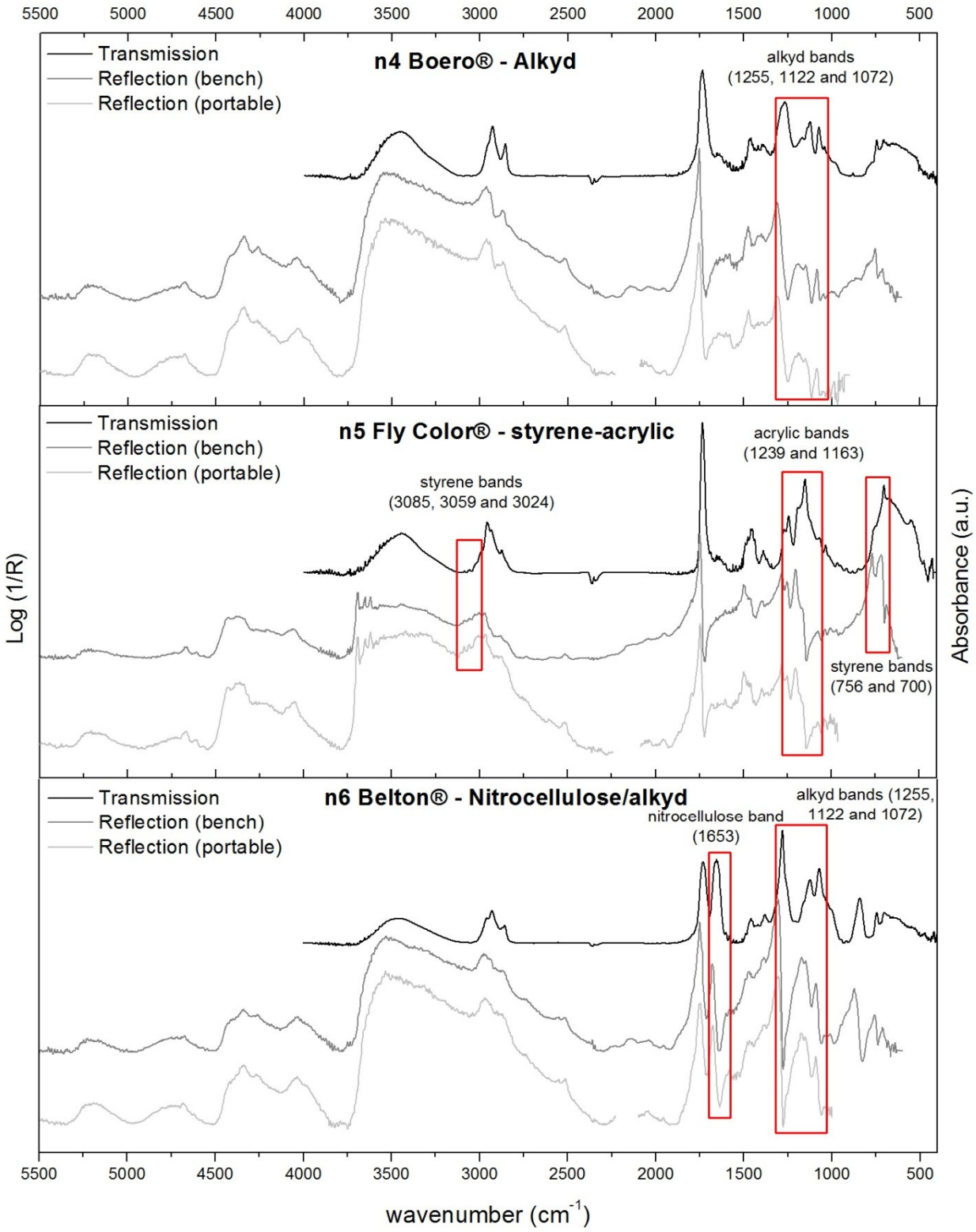

Figure a4 (cont.) – FTIR spectra of all commercial white paint formulations studied where binders were indentified. The spectra are presented in transmission and in reflection mode (with bench and portable equipment), for each white paint. The most important bands are assigned for each binder.

- Chemical cleaning. This experiment was performed by a well-experienced conservator in modern and contemporary paintings area. For this experiment pure solvents and chemical systems were used giving a total of eight products. Pure solvents are presented in table a2. As for the chemical systems, ammonium (NH_4OH, 6% in water) and deionized water were used, from supplier CTS Srl (Italy).

Table a2 – Pure organic solvents used in the cleaning of mock-up #6.

White ground	Description	Assay (%)	Supplier
n6 Belton®	Acetone	≥ 99.5%	CTS Srl (Italy)
	Ethanol	≥ 95%	
	Isopropyl alcohol	87 - 91% Isopropyl Alcohol 10 - 12% Isobutyl Alcohol	
	Xylene	≥ 98%	
	Petroleum ether 80-100°C	-	
	Ethyl L-Lactate	98%	

All solvents and chemical systems were applied in each paint layer using a cotton swab. The cleaning duration was approximately the same, as well as the concentration used in the cotton swab controlled by conservator's sensitivity.

- Laser cleaning parameters. The lasers used are laboratory systems or systems specially developed by the Institute of Electronic Structure & Laser, Foundation for Research and Technology-Hellas (FORTH-IESL). The employed cleaning regimes are frequently used for conservation interventions. The laser systems used were one KrF excimer laser (Lambda Physik - LPX 200) working at 248 nm (t_p = 30 ns) and two different Q-switched Nd:YAG lasers: a Specton Laser System SL805 using wavelength at 1064 nm, 532 nm and 355 nm (t_p = 10 ns); and an Elen Palladio laser at 355 nm (t_p = 150 ps), therefore using wavelengths from UV to infrared.

The laser cleaning experiment was conducted at the FORTH-IESL, in Greece. The ablation process was applied for each paint combination in a regime of spots or scanning lines, in order to eliminate the outer layer without compromise the white ground. The laser cleaning experimental details for each canvas are showed in table a3.

Table a3 – Laser cleaning general parameters used for each mock-up.

mock-up	White ground	Laser system	Wavelength (nm)	Pulse length	Shape	Ablation area (mm)	Energy density ($J \cdot cm^{-2}$)	number of pulses
#1	**n1** Polycolor®	Nd:YAG	1064	10 ns	rounded spots	2.8 x 3.7	0.50 to 3.02	1-5
			532	10 ns		2.8 x 2.6	0.10 to 1.45	1-10
			355	10 ns		1.7 x 1.9	0.08 to 2.06	1-10
				150 ps		1.4 x 1.4	1.40 to 2.04	1-21
		KrF Excimer	248	30 ns	scanning lines	0.7 x 12	1.49 to 3.06	1-60
#2	**n2** Liquitex®	KrF Excimer	248	30 ns	scanning lines	1.35 x 5.2	4.43 to 5.00	1-50

Table a3 (cont.) – Laser cleaning general parameters used for each mock-up.

mock-up	White ground	Laser system	Wavelength (nm)	Pulse length	Shape	Ablation area (mm)	Energy density ($J \cdot cm^{-2}$)	number of pulses
#3	**n3** Griffin®	KrF Excimer	248	30 ns	scanning lines forming squares	120 x 120	1.79	12-34
#4	**n4** Boero®	KrF Excimer	248	30 ns	scanning lines	0.7 x 12 1.35 x 5.2	3.06 to 4.99	1-60
				30 ns	scanning lines forming squares	120 x 120	1.79	44/50
		Nd:YAG	355	150 ps	rounded spots	1.4 x 1.4	0.81 to 2.04	1-30

- Bench top equipments

Optical Microscopy

The painting mock-ups were observed under a Leica DMRX Optical Microscope equipped with a Digital Camera Leica DC 300. Images were capture in reflection using polarized visible light.

FTIR Spectroscopy

FTIR analyses in transmission mode were carried out using a JASCO FT/IR-4100 FTIR spectrometer, composed by a ceramic light source, Michelson interferometer and a DLATGS detector. All spectral measurements were acquired in absorption mode with an effective range of 4000–400cm^{-1} and at a resolution of 2 cm^{-1}. All powdered samples were prepared with finely ground potassium bromide pellets, using a manual hydraulic press, and a background correction using the alone pressed KBr pellet. Spectra were obtained over 100 scansions.

For the FTIR analyses in reflection mode a JASCO IMV 4000 FTIR spectrometer was used, equipped with a nitrogen cooled MCT (Mercury Cadmium Telluride) detector and an IRT-30 optical microscope. Measurements were performed directly on the surface of the samples with a Cassegrain 16x objective. A background was performed every two spectra obtained. The spectra were recorded covering the wavenumber range 6000-600 cm^{-1} with a spectral resolution of 4 cm^{-1}. The total reflectivity R was collected over 800 scansions using the spectrum from an aluminium mirror plate for background correction. Spectra were expressed as function of pseudo-absorbance A' where A' = log (1/R).

Raman Spectroscopy

Raman spectra were obtained using a JASCO Ventuno double grating spectrophotometer equipped with a CCD detector cooled at −48 ºC and coupled to an optical microscope. Raman spectra were excited using the green line (at 532 nm) of a Nd:YAG laser. Laser power at the sample was kept between 0.4 and 4.3 mW, the exposition time varied between 7 s to 30 s with 5 to 10 accumulations. The spectra were recorded with the wavenumber range 4800-50 cm^{-1} and the resolution was about 2 cm^{-1}. The spectrometer calibration was accomplished using the Raman lines of a polystyrene and a sulphur standard.

- Portable equipments

Fibre-optics video microscopy

A fibre-optics video microscope was used, which is composed by a Halogen light source, and a CCD camera. The objective used (50x) works in contact mode.

X-ray fluorescence

The XRF spectra were recorded using portable equipment made with a miniaturized X-ray generator EIS P/N 9910, equipped with a tungsten anode and a silicon drift detector (SDD) cooled with a Peltier element. The SDD has a resolution of about 150 eV at 5.9 keV. The portable instrument allows the detection of elements with atomic number higher than silicon (Z > 14). The excitation parameters used during the measurements were: voltage of 38 kV and current of 0.05 mA. The acquisition time was 120 s. The distance sample-detector was fixed at 2 cm. The beam diameter under these conditions is 4 mm.

Fibre-optics UV-vis-NIR reflectance spectrophotometry

Reflectance spectra were obtained by a portable spectrophotometer. The reflected light is converged by a fibre-optic cable to a high sensitivity Avantes CCD spectrometer (86 photons/counting, 200–1100 nm, grating 300 lines/mm). The excitation source is a deuterium-halogen lamp (AvaLight-D(H)-S) and an integrating sphere with a 6 mm viewing aperture (AvaSphere-30-refl, internal diameter 30 mm) is used to collect and to transfer the reflectance signals to the detector.

Fibre-optics FTIR spectroscopy

A portable JASCO VIR 9500 spectrophotometer equipped with a Remspec mid-infrared fibre optic sampling probe was used. It is composed of a Midac Illuminator IR radiation source, a Michelson interferometer and a liquid nitrogen cooled MCT-detector. The probe is a bifurcated cable containing 19 chalcogenide glass fibres that allows the collection of spectra in the range 7000–900 cm^{-1} at a resolution of 4 cm^{-1}. The probe diameter is about 4 mm. The total reflectivity, R, due to the combined diffuse and specular components, was collected over 800 scansions using the spectrum from an aluminium mirror plate for background correction. Spectra were expressed as function of pseudo-absorbance A' where A' = log(1/R).

Fibre-optics Raman spectroscopy

The portable instrument is a fibre-optics micro-Raman Jasco prototype, assembled from various commercial components, that weights about 25 kg. The laser source is the green line (532 nm) of a portable Nd:YAG. The laser radiation is focused through an optical fibre (2 m long and 100 μm diameter) into a JASCO RMP-100 microprobe equipped with an Olympus objective. The laser power at the sample was a maximum of about 30 mW. The compact spectrograph is equipped with a Czerny-Turner polychromator of about 100 mm of focal length, with manual scansion, manual change of gratings. The detector is a multichannel CCD cooled at -50ºC. The portable set up has a spectral resolution of about 8 cm^{-1}. It can also be equipped with a diode laser at 785 nm.

Appendix 2 – Photocatalytic properties of titanium dioxide

Titanium dioxide (TiO_2) belongs to the family of transition metal oxides having titanium in oxidation state IV. It exists in several crystalline forms, to mention the most relevant, the anatase and rutile forms, being this last one the most stable one. It is a semiconductor metal, and, thus, its HOMO is named valence band (VB) and its LUMO named conduction band (CB) [1,2].

The differences in the crystalline structures of anatase and rutile lead to different band gaps: anatase 3.20 eV and rutile 3.02 eV. Both are commonly used as photocatalysts, with anatase showing a greater photocatalytic activity. A photocatalyst is capable to adsorb simultaneously two reactants, which can be reduced and oxidized by a photonic activation through an efficient absorption ($h\nu \geq Eg$). The absorption thresholds in wavelength are 384 nm for anatase and 410 nm for rutile [1]. The photocatalysis electronic process depends on the promotion of an electron to the CB, upon irradiation by UV light, resulting in a "hole" in the VB [1,2], as summarized in the following reaction.

$$TiO_2 + h\nu \rightarrow h_{VB}^{+} + e_{CB}^{-} \text{ (charge separation) [2]}$$

The most active field of TiO_2 photocatalysis is the photodegradation of organic compounds, being due to these highly oxidizing holes and the resulting hydroxyl radicals ($HO^{\bullet}$) [1]. The hole in the VB has the potential to oxidize water resulting in the formation of these $HO^{\bullet}$ [2] as shown the reaction below.

$$h_{VB}^{+} + H_2O \rightarrow OH^{\bullet} \text{ ($OH^{\bullet}$ generation - VB) [2]}$$

Since in the CB the electron has no more a hole to recombine with, it reduces oxygen to form a superoxide anion, which can react with water and form again the hydroxyl radical ($HO^{\bullet}$) [2]

$$e_{CB}^{-} + O_2 \rightarrow O_2^{\bullet -} + H_2O \rightarrow OH^{\bullet} \text{ ($OH^{\bullet}$ generation - CB) [2]}$$

Practically, every functional group with either a non-bonded lone pair or p-conjugation may exhibit an oxidative reactivity towards TiO_2, undergoing dehydrogenation, oxygenation, or oxidative cleavage [1].

[1] Carp, O., Huisman, C. L., Reller, A., 'Photoinduced reactivity of titanium dioxide', *Progress in Solid State Chemistry* **32** (2004) 33-177.

[2] Seery, M., 'Metal Oxide Photocatalysis', in *The Photochemistry Portal - Principles, Applications and Experimentation in Modern Photochemistry* (30th September 2009), retrieved in July 13, 2010 from: http://photochemistryportal.net/home/index.php/tag/titanium-dioxide/

Table a4 - Results for the laser cleaning experiment on mock-up #1 using different laser systems.

Laser system	1. Polycolor®	2. Liquitex®	3. Griffin®
KrF Excimer λ= 248 nm t_p= 30 ns	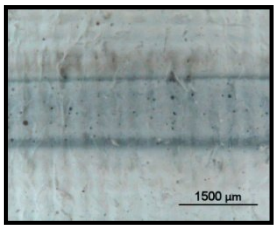 *Fluence=2.3 J·cm^{-2}, 10p* Removal was not possible & discoloration	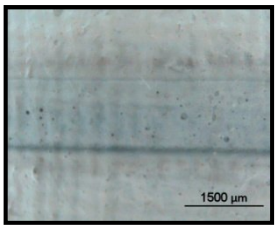 *Fluence=2.3 J·cm^{-2}, 10p* Removal was not possible & overpaint discoloration	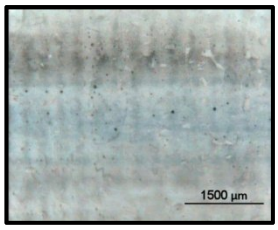 *Fluence=3.0 J·cm^{-2}, 10p* Removal was not possible & overpaint discoloration
Nd:YAG λ= 355 nm t_p=10 ns	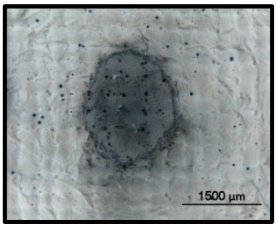 *Fluence=2.0 J·cm^{-2}, 10p* Removal was not possible & intense discoloration	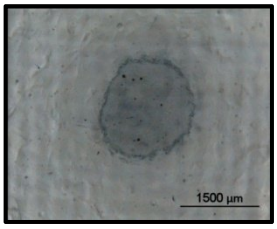 *Fluence=1.2 J·cm^{-2}, 5p* **Overpaint removal** BUT with discoloration	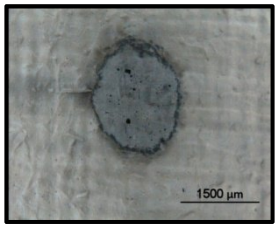 *Fluence=2.0 J·cm^{-2}, 10p* **Overpaint removal** BUT intense discoloration & black halo
Nd:YAG λ= 355 nm t_p=150 ps	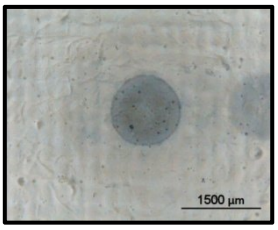 *Fluences=2.0 J·cm^{-2}, 5p* Removal was not possible & discoloration	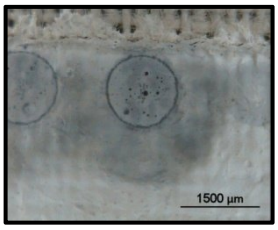 *Fluence=1.4 J·cm^{-2}, 20p* Partial removal & discoloration with black halo	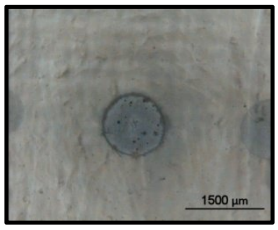 *Fluence=2.0 J·cm^{-2}, 10p* Partial removal & discoloration
Nd:YAG λ= 532 nm t_p=10 ns	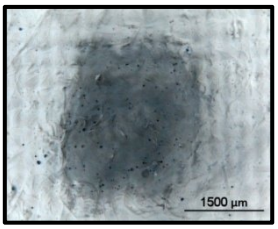 *Fluence=1.4 J·cm^{-2}, 3p* Removal was not possible & intensive discoloration	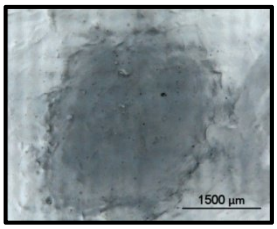 *Fluence=1.0 J·cm^{-2}, 5p* Partial cleaning & intense discoloration	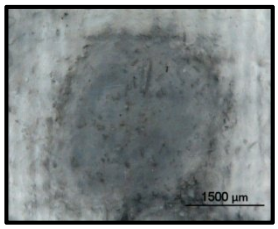 *Fluence=1.0 J·cm^{-2}, 5p* Partial cleaning & intense discoloration
Nd:YAG λ= 1064 nm t_p=10 ns	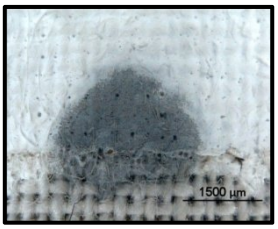 *Fluence=3.0 J·cm^{-2}, 1p* Removal was not possible & intensive discoloration	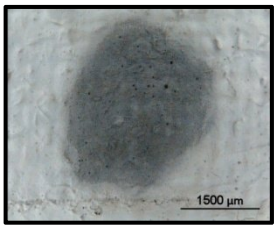 *Fluence=2.4 J·cm^{-2}, 1p* Removal was not possible & intensive discoloration	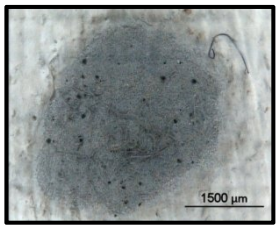 *Fluence=2.4 J·cm^{-2}, 3p* Aggressive ablation with discoloration & damage

Table a4 (cont.) - Results for the laser cleaning experiment on mock-up #1 using different laser systems.

Laser system	4. Boero®	5. Fly Color®	6. Belton®
KrF Excimer λ= 248 nm t_p= 30 ns	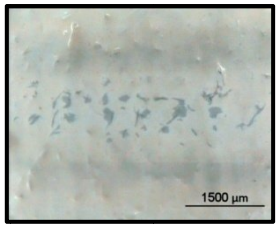 *Fluence=3.0 J·cm^{-2}, 10p* Removal was not possible & overpaint and ground discoloration	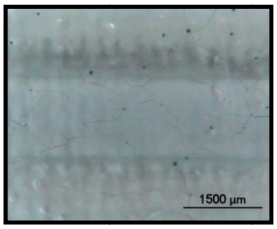 *Fluence=3.0 J·cm^{-2}, 10p* Removal was not possible & overpaint discoloration	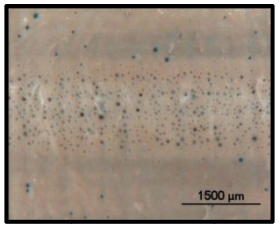 *Fluence=3.0 J·cm^{-2}, 20p* Removal was not possible
Nd:YAG λ= 355 nm t_p=10ns	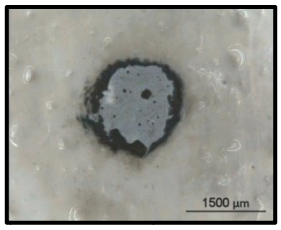 *Fluence=2.0 J·cm^{-2}, 10p* **Overpaint removal** BUT with discoloration & black halo around the ablated area	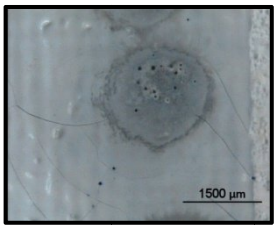 *Fluence=2.0 J·cm^{-2}, 5p* Partial removal & discoloration	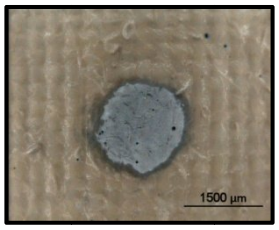 *Fluence=2.0 J·cm^{-2}, 10p* **Overpaint removal** BUT with discoloration & black halo around the ablated area
Nd:YAG λ= 355 nm t_p=150 ps	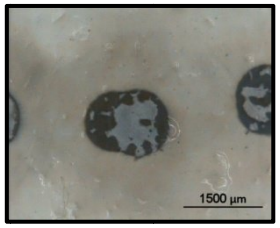 Fluence=2.0 *J·cm^{-2}*, 10p **Overpaint removal** BUT discoloration	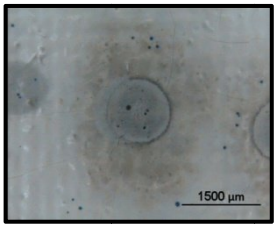 *Fluence=2.0 J·cm^{-2}, 20p* **Overpaint removal** BUT with discoloration	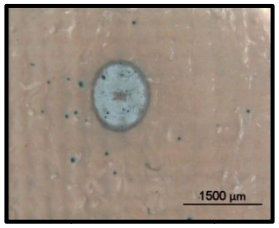 *Fluence=2.0 J·cm^{-2}, 10p* **Overpaint removal** with some residues & slight discoloration
Nd:YAG λ= 532 nm t_p=10 ns	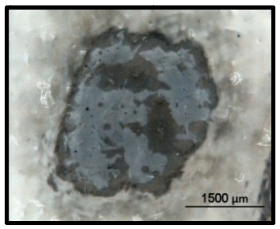 *Fluence=1.0 J·cm^{-2}, 10p* Partial cleaning & intensive discoloration with black halo around the ablated area	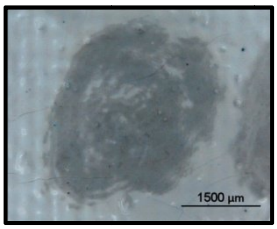 *Fluence=1.0 J·cm^{-2}, 3p* Removal was not possible & overpaint discoloration	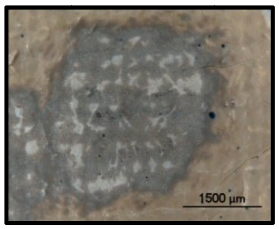 *Fluence=1.4 J·cm^{-2}, 1p* Partial cleaning & discoloration
Nd:YAG λ= 1064 nm t_p=10 ns	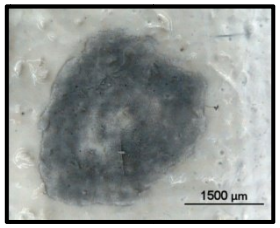 *Fluence=2.4 J·cm^{-2}, 1p* Aggressive ablation with discoloration & damage	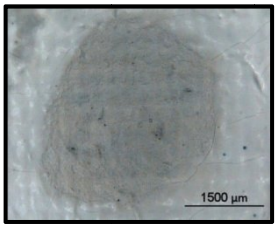 *Fluence=2.8 J·cm^{-2}, 1p* Removal was not possible & overpaint discoloration	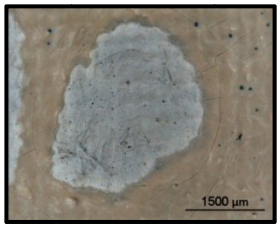 *Fluence=3.0 J·cm^{-2}, 1p* Partial cleaning & slight discoloration

Table a4 (cont.) - Results for the laser cleaning experiment on mock-up #1 using different laser systems.

Laser system	7. Polycolor®	8. Liquitex®	9. Griffin®
KrF Excimer λ= 248 nm t_p= 30 ns	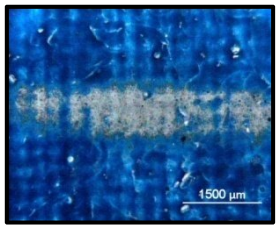 *Fluence=3.0 J·cm^{-2}, 20p* **Overpaint removal** BUT with slight discoloration	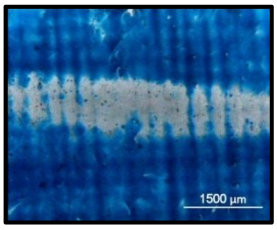 *Fluence=3.0 J·cm^{-2}, 10p* **Overpaint removal** BUT with slight discoloration	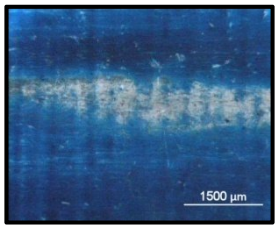 *Fluence=3.0 J·cm^{-2}, 20p* **Overpaint removal** BUT with slight discoloration
Nd:YAG λ= 355 nm t_p=10 ns	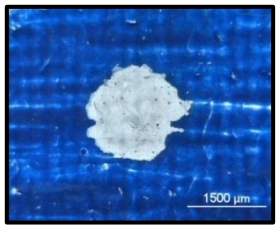 *Fluence=2.0 J·cm^{-2}, 10p* **Overpaint removal**	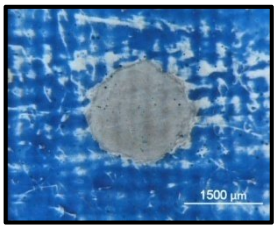 *Fluence=2.0 J·cm^{-2}, 10p* **Overpaint removal** BUT with discoloration	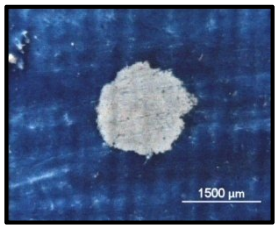 *Fluence=2.0 J·cm^{-2}, 10p* **Overpaint removal** & slight discoloration
Nd:YAG λ= 355 nm t_p=150 ps	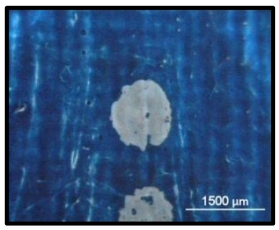 *Fluence=2.0 J·cm^{-2}, 10p* **Overpaint removal** & slight discoloration	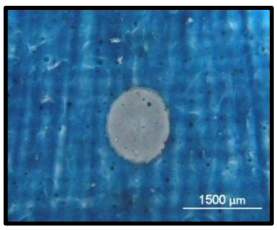 *Fluence=2.0 J·cm^{-2}, 10p* **Overpaint removal** & slight discoloration	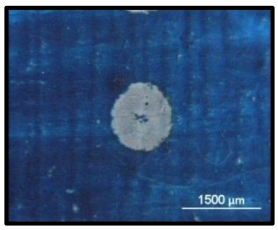 *Fluence=2.0 J·cm^{-2}, 10p* **Overpaint removal** with some residues & slight discoloration
Nd:YAG λ= 532 nm t_p=10 ns	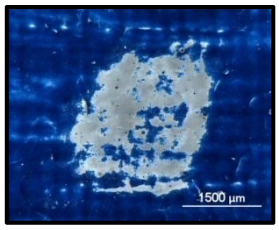 *Fluence=1.0 J·cm^{-2}, 5p* Partial cleaning & slight discoloration	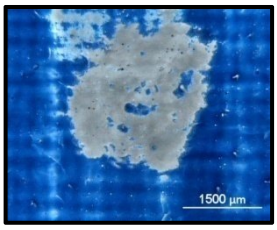 *Fluence=1.0 J·cm^{-2}, 5p* **Overpaint removal** BUT with slight discoloration	not tested
Nd:YAG λ= 1064 nm t_p=10 ns	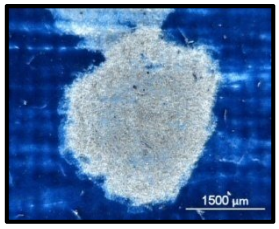 *Fluence=3.0 J·cm^{-2}, 3p* Aggressive ablation with slight discoloration & damage	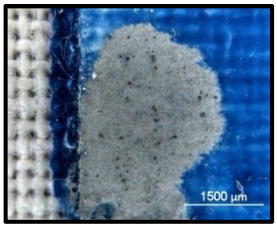 *Fluence=3.0 J·cm^{-2}, 3p* Aggressive ablation with discoloration & damage	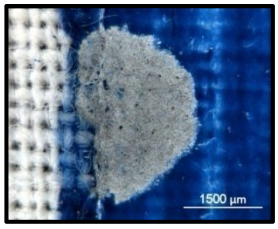 *Fluence=3.0 J·cm^{-2}, 3p* Aggressive ablation with discoloration & damage

Table a4 (cont.) - Results for the laser cleaning experiment on mock-up #1 using different laser systems.

Laser system	10. Boero®	11. Fly Color®	12. Belton®
KrF Excimer λ= 248 nm t_p= 30 ns	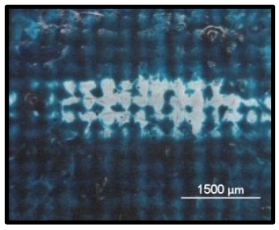 *Fluence=3.0 J·cm^{-2}, 20p* Partial cleaning	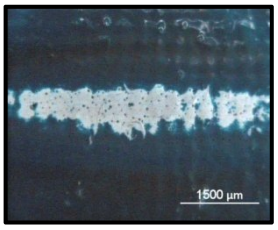 *Fluence=3.0 J·cm^{-2}, 60p* **Overpaint removal**	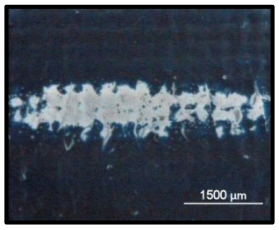 *Fluence=3.0 J·cm^{-2}, 20p* **Overpaint removal**
Nd:YAG λ= 355 nm t_p=10 ns	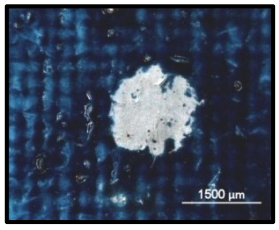 *Fluence=2.0 J·cm^{-2}, 10p* **Overpaint removal** & slight discoloration	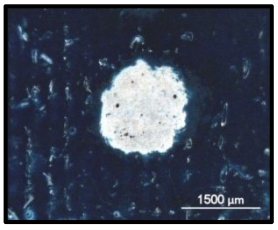 *Fluence=2.0 J·cm^{-2}, 10p* **Overpaint removal**	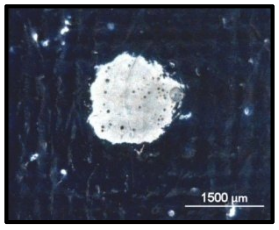 *Fluence=2.0 J·cm^{-2}, 10p* **Overpaint removal**
Nd:YAG λ= 355 nm t_p=150 ps	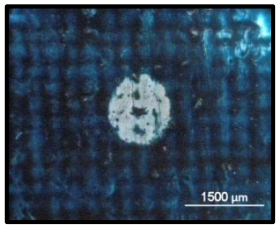 *Fluence=2.0 J·cm^{-2}, 10p* **Overpaint removal** with some residues	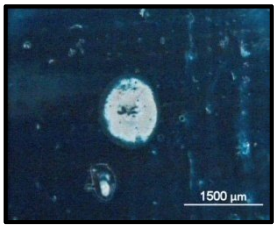 *Fluence=2.0 J·cm^{-2}, 10p* **Overpaint removal** with some residues	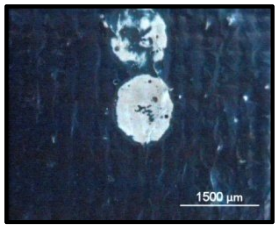 *Fluence=2.0 J·cm^{-2}, 10p* **Overpaint removal** with some residues
Nd:YAG λ= 532 nm t_p=10 ns	not tested	not tested	not tested
Nd:YAG λ= 1064 nm t_p=10 ns	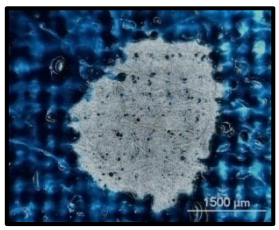 *Fluence=3.0 J·cm^{-2}, 3p* Aggressive ablation with discoloration & damage	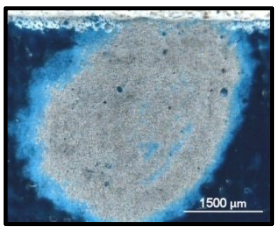 *Fluence=1.1 J·cm^{-2}, 5p* Aggressive ablation with discoloration & damage	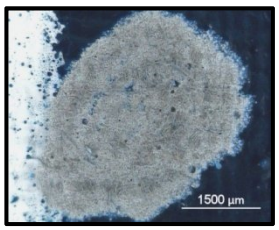 *Fluence=1.1 J·cm^{-2}, 5p* Aggressive ablation with discoloration & damage

Table a5 - Results for the laser cleaning experiment on mock-up #4 using different laser systems.

Laser system	1. Polycolor®	2. Liquitex®	3. Griffin®
KrF Excimer λ= 248 nm t_p= 30 ns	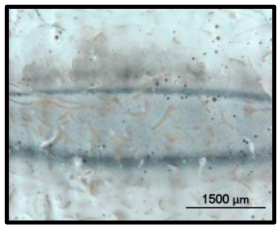 *Fluence=3.0 J·cm^{-2}, 20p* Partial cleaning with overpaint discoloration	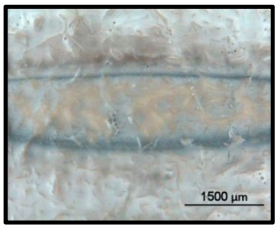 *Fluence=3.0 J·cm^{-2}, 15p* Partial cleaning with overpaint discoloration	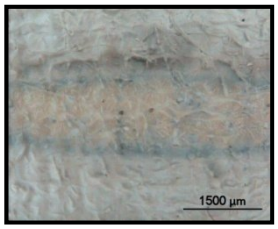 *Fluence=3.0 J·cm^{-2}, 30p* Partial cleaning with overpaint discoloration
	4. Boero®	**5. Fly Color®**	**6. Belton®**
	not tested	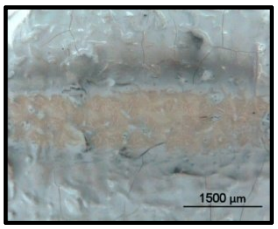 *Fluence=3.0 J·cm^{-2}, 40p* Partial cleaning & overpaint discoloration	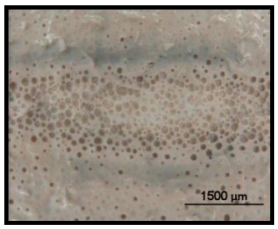 *Fluence=3.0 J·cm^{-2}, 40p* Aggressive cleaning & damage
	7. Polycolor®	**8. Liquitex®**	**9. Griffin®**
	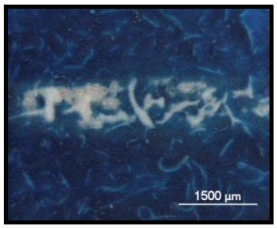 *Fluence=3.0 J·cm^{-2}, 30p* Partial cleaning	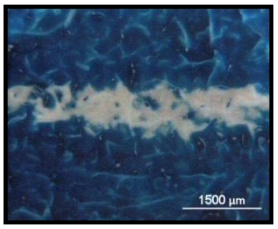 *Fluence=3.0 J·cm^{-2}, 15p* **Overpaint removal** with some residuals	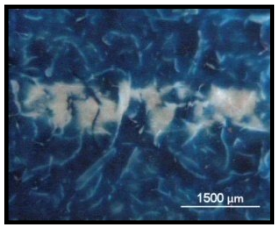 *Fluence=3.0 J·cm^{-2}, 20p* Partial cleaning
	10. Boero®	**11. Fly Color®**	**12. Belton®**
	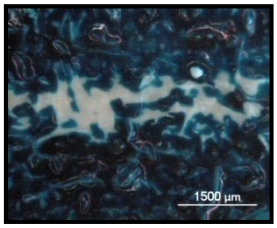 *Fluence=3.0 J·cm^{-2}, 30p* Partial cleaning	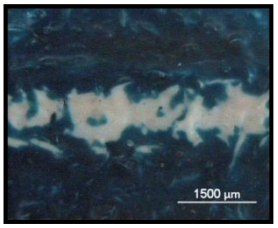 *Fluence=3.0 J·cm^{-2}, 30p* **Overpaint removal** with some residuals	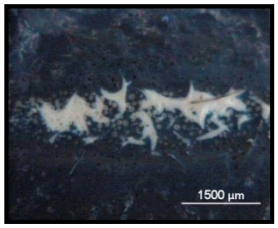 *Fluence=3.0 J·cm^{-2}, 40p* Partial cleaning & damage

Table a5 (cont.) - Results for the laser cleaning experiment on mock-up #4 using different laser systems.

Laser system	1. Polycolor®	2. Liquitex®	3. Griffin®
Nd:YAG λ= 355 nm t_p=150 ps	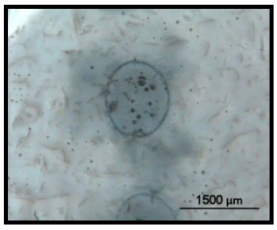 *Fluence=1.4 J·cm^{-2}, 15p* Partial cleaning with discoloration	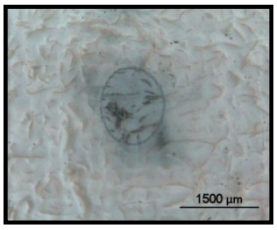 *Fluence=1.4 J·cm^{-2}, 10p* Partial cleaning with discoloration & canvas exposure	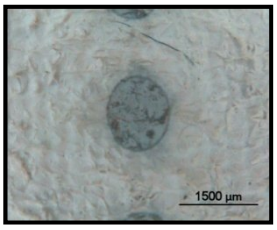 *Fluence=1.4 J·cm^{-2}, 9p* Partial cleaning with discoloration & canvas exposure
	4. Boero®	**5. Fly Color®**	**6. Belton®**
	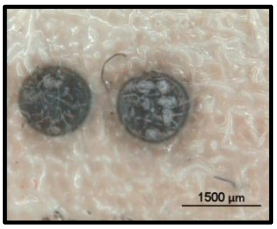 *Fluence=1.4 J·cm^{-2}, 20p* **Overpaint removal** BUT with discoloration and damage	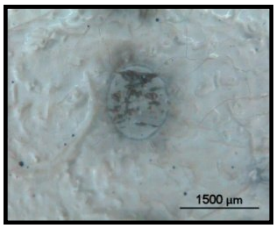 *Fluence=1.4 J·cm^{-2}, 10p* Partial cleaning with discoloration & canvas exposure	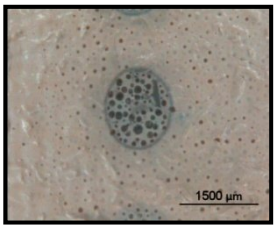 *Fluence=1.4 J·cm^{-2}, 10p* Aggressive cleaning with discoloration and canvas exposure
	7. Polycolor®	**8. Liquitex®**	**9. Griffin®**
	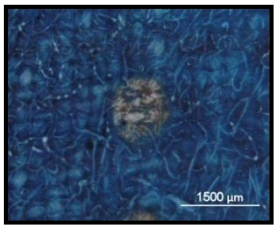 *Fluence=1.4 J·cm^{-2}, 10p* Aggressive cleaning with discoloration & canvas exposure	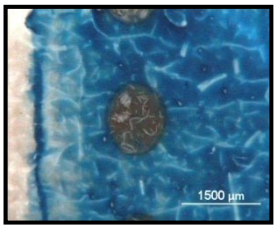 *Fluence=1.4 J·cm^{-2}, 10p* Aggressive cleaning with discoloration & canvas exposure	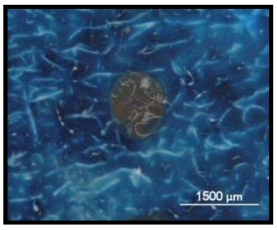 *Fluence=1.4 J·cm^{-2}, 10p* Aggressive cleaning with discoloration & canvas exposure
	10. Boero®	**11. Fly Color®**	**12. Belton®**
	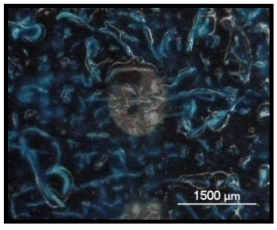 *Fluence=1.4 J·cm^{-2}, 20p* Aggressive cleaning with discoloration & canvas exposure	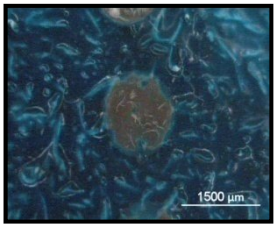 *Fluence=1.4 J·cm^{-2}, 10p* Aggressive cleaning with discoloration & canvas exposure	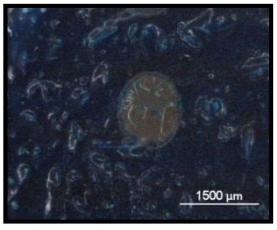 *Fluence=1.4 J·cm^{-2}, 20p* Aggressive cleaning with discoloration & canvas exposure

Appendix 4 – Participation on conferences

Domingues, J., Rosi, F., De Cesare, G., Miliani, C., 'Spectroscopy studies on conservation issues in modern and contemporary art paintings' (oral presentation), in *Youth in Conservation of Cultural Heritage (Yococu 2010)*, Palermo (Italy), 24-26 May 2010.

De Cesare, G., Melessanaki, K., Pouli, P., Domingues, J., Rosi, F., Miliani, C., Fotakis, C., 'Laser cleaning applied to contemporary paintings: optimization of working parameters' (poster presentation), in *New insights into the cleaning of paintings (Cleaning 2010)*, Universidad Politécnica de Valencia (Spain), 26-28 May 2010.

De Cesare, G., Melessanaki, K., Pouli, P., Domingues, J., Rosi, F., Miliani, C., Fotakis, C., 'Il laser nella pulitura delle pitture contemporanee: selezione dei parametri operativi' (oral presentation), in *Applicazione laser nel restauro (Aplar3)*, Bari (Italy), 18-19 June 2010.

De Cesare, G., Melessanaki, K., Pouli, P., Domingues, J., Rosi, F., Miliani, C., Fotakis, C., 'Contemporary art paintings: a study on the laser assisted removal of past and unsuccessful retouches' (oral presentation), in *Fundamentals of Laser Assisted Micro- & Nanotechnologies (FLAMN-10)*, St. Petersburg (Russia) 5-8 July 2010.

Domingues, J., Rosi, F., De Cesare, G., Miliani, C., 'Spectroscopy studies on conservation issues in modern and contemporary art paintings' (poster presentation), in *4th Intensive School on Conservation Science,* Teruel (Spain), 19-30 July 2010.